PHYSICAL REVIEW D **88,** 044048 (2013)

$f(R, T)$ cosmological models in phase space

Hamid Shabani* and Mehrdad Farhoudi†

Department of Physics, Shahid Beheshti University, G.C., Evin, Tehran, 19839, Iran

(Received 25 June 2013; published 26 August 2013)

We investigate the cosmological solutions of $f(R, T)$ modified theories of gravity for a perfect fluid in a spatially Friedmann-Lemaître-Robertson-Walker metric through the phase-space analysis, where R is the Ricci scalar and T denotes the trace of the energy-momentum tensor of the matter content. We explore and analyze the three general theories with the Lagrangians of minimal $g(R) + h(T)$, pure nonminimal $g(R)h(T)$, and nonminimal $g(R)(1 + h(T))$ couplings through the dynamical systems approach. We introduce a few variables and dimensionless parameters to simplify the equations to more concise forms. The conservation of the energy-momentum tensor leads to a constraint equation that, in the minimal gravity, confines the functionality of $h(T)$ to a particular form, and hence relates the dynamical variables. In this case, acceptable cosmological solutions that contain a long enough matter-dominated era followed by a late-time accelerated expansion are found. To support the theoretical results, we also obtain numerical solutions for a few functions of $g(R)$, and the results of the corresponding models confirm the predictions. We separate the solutions into six classes which demonstrate more acceptable solutions and there is more freedom to have the matter-dominated era than in $f(R)$ gravity. In particular, there is a new fixed point which can represent the late-time acceleration. We draw different diagrams of the matter densities (consistent with the present values), the related scale factors, and the effective equation of state. The corresponding diagrams of the parameters illustrate that there is a saddle acceleration era which is a middle era before the final stable-acceleration de Sitter era for some models. All presented diagrams determine radiation, matter, and late-time acceleration eras very well. The pure nonminimal theory suffers from the absence of a standard matter era, though we illustrate that the nonminimal theory can have acceptable cosmological solutions.

DOI: 10.1103/PhysRevD.88.044048 PACS numbers: 04.50.Kd, 95.36.+x, 98.80.−k, 98.80.Jk

I. INTRODUCTION

Since the birth of general relativity (GR) in 1915, the theory has faced the appearance of new ideas seeking to change or even replace it in favor of an alternative one[1] which could solve different aspects or at least some parts of its incompleteness and shortcomings. These novel ideas mainly consist of some modifications or generalizations which would challenge GR in a geometrical background. Some of these theories introduce extra dimensions, e.g., the Kaluza–Klein theories [3] and braneworld scenarios [4]. Other alternatives are scalar-tensor theories, e.g., the Brans–Dicke theory [5] and higher-order/modified gravities [2,6–12]. Another possibility is to introduce some new cosmic fluids, e.g., dark matter [13–17], which should give rise to clustered structures, and dark energy [18–22], which is responsible for the observed accelerated expansion of the Universe. In particular, the fundamental incompatibility with quantum theory and the observational inability to explain the flatness of galaxy rotation curves [23,24] can be regarded as insufficiencies of GR. Also, the existing problems of the isotropic and homogeneous cosmological solution of GR (the standard big bang cosmology), such as the horizon and the flatness problems [25], and the absence of solutions including the well-accepted states of cosmological evolution in the past and future, namely, an accelerating-phase solution prior to the radiation-dominated era, e.g., inflation [26–30], and an acceleration phase needed to explain the present accelerated expansion observed by, e.g., type Ia supernovae (SNIa) observations [31–35], large-scale structure [36,37], baryon acoustic oscillations [38–40], the cosmic microwave background radiation (CMBR) [41–43], and weak lensing [44]. Of course, in spite of the above deficiencies, GR has had many successes, such as matching the experimental results for the precession of Mercury's orbit [45–47], the Lense–Thirring gravitomagnetic precession [48], the gravitational deflection of light by the sun [45–47], and the gravitational redshift[2] [45–47]. On the whole, the results of Einstein's theory when considering the development of a general phenomenological framework, i.e., the parametrized post-Newtonian formalism, determine that it is the best known metric theory of gravity [46].

Among the extended theories of gravity, there are at least two main motivations[3] for employing the higher-order gravities, i.e., those in which the Einstein-Hilbert

*h_shabani@sbu.ac.ir
†m-farhoudi@sbu.ac.ir

[1]For example, see Refs. [1,2] and references therein.

[2]However, any relativistic theory of gravitation consistent with the principle of equivalence will predict a redshift.

[3]See, e.g., Ref. [6].

action is modified by higher-order curvature invariants with respect to the Ricci scalar. The first motivation has a theoretical background and is related to the nonrenormalizability of GR [49,50] and to the fact that GR cannot be quantized conventionally. Regarding this issue, some authors have shown that the inclusion of higher-order terms can solve this problem [51,52]. The other motivation is related to the recently achieved data in astrophysics and cosmology. Two contemporary pieces of evidence, which are referred to as dark matter and dark energy, have challenged our knowledge about the Universe and have accounted for the first signals of a breakdown of GR. It is also worth mentioning that the concordance or ΛCDM model [53]—the simplest model which adequately fits the present observations and is supported by an inflation scenario[4]—can account for an accelerating phase in the very early and late Universe. However, the ΛCDM model suffers from the well-known cosmological problem originating from the cosmological constant pertaining to the vacuum energy [54–56]. That is, the cosmological constant is tremendously small with respect to the vacuum energy that is defined in particle physics. With regard to this, a mechanism is needed to get such a small value to match the present observations, and dynamical dark energy models contain such mechanisms [57,58].

$f(R)$ gravities, as the simplest family of the higher-order gravities, are obtained by replacing the Ricci scalar with a function $f(R)$ in the Einstein-Hilbert action. Generally, every new gravity theory introduced as an alternative to GR should be tested in two realms; that is, the weak-field tests, i.e., those that can elaborate whether the theory leads to the known Solar System observations, and the cosmological tests which inspect the theory to find at least a solution that matches the present accelerated expansion observations. $f(R)$ gravity theories are not excepted from these examinations. With regard to these issues, a few authors have claimed that the Solar System tests rule out most $f(R)$ models [59–61], though others do not agree with these results [8]. However, these issues do not seem to be settled completely; see, e.g., Refs. [9,12]. Despite the results of local gravity tests, one can still look at these theories for cosmological solutions as an independent criterion [62]. In this sense, these theories can be considered as $f(R)$ dark energy models, implying that they can play the role of dark energy without using a cosmological constant, i.e., they can encompass these problems in a self-consistent scheme. Nevertheless, in addition to $f(R)$ gravities, there are numerous alternative gravity theories that claim to cure the problems of dark energy and inflation, in which—up to now—most of the physical content of these theories has been widely explored; see, e.g., Refs. [2,22].

In this work, we purpose to study the cosmology of the so-called $f(R, T)$ gravity, first introduced in Ref. [63] and studied in Refs. [64–71]. The theory of $f(R, T)$ gravity generalizes $f(R)$ theories of gravity by the incorporation of the trace of the energy-momentum tensor in addition to the Ricci scalar. The justification for the dependence on T comes from inductions arising from some exotic fluid and/or quantum effects (conformal anomaly[5]). Actually, this induction point of view adopts or links with the known proposals, such as geometrical curvature inducing matter, a geometrical description of physical forces, and a geometrical origin for the matter content of the Universe.[6] In Ref. [63], the field equations of some particular models were presented, and in particular scalar field models $f(R, T^{\phi})$ were analyzed in detail with a brief consideration of their cosmological implications. Also, the equation of motion of the test particle and the Newtonian limit of this equation were further analyzed in Ref. [63]. Up to now, the issues which have been investigated along with this modified theory are the energy conditions [65], thermodynamics [66–68], anisotropic cosmology [69], the cosmology in which the representation employs an auxiliary scalar field [64], the reconstruction of some cosmological models [70], and scalar perturbations [71]. Also, a further generalization of this theory has been proposed recently in Refs. [73,74]. Incidentally, in the literature authors have worked on a theory of gravity called "the $f(T)$ gravity" (see, e.g., Ref. [75] and references therein), where T in this theory is the torsion scalar arising from the torsion tensor in a similar way as the curvature scalar arises from the curvature tensor, and which is completely different from $f(R, T)$ gravity.

On the other hand, $f(R, T)$ gravity may be considered as a correction or generalization of $f(R)$ gravities as long as cosmological considerations are addressed. In this regard, we employ $f(R, T)$ gravity in an extended version of (and with terminology similar to) $f(R)$ gravity employed in Ref. [76]. Hence, in the forthcoming sections, we theoretically investigate the cosmological solutions of $f(R, T)$ models and compare the results with the corresponding $f(R)$ cosmological models of Ref. [76]. To support the theoretical results, we also obtain numerical solutions. In Sec. II, we derive the equations of motion (EOM) for $f(R, T)$ gravity and show that in this case the conservation of the energy-momentum tensor leads to a constraint equation that must be satisfied by any function of $f(R, T)$. For example, a minimal coupling of the form $f(R, T) = g(R) + h(T)$ restricts the form of the function $h(T)$. Then, we introduce a number of variables to simplify the equations for later applications. In Sec. III, we analyze the

[4]Such a scenario is needed because the accelerated phase in the very early Universe should end to connect to a radiation-dominated phase; however, a cosmological constant cannot fulfill this requirement [25].

[5]See, e.g., Refs. [49,72].

[6]See, e.g., Refs. [1,72] and references therein.

cosmological solution through the dynamical systems approach. We also consider the minimal combination, and obtain the corresponding solutions and the conditions for the existence of acceptable solutions. In Sec. IV, we investigate the numerical results for several functions of $f(R,T)$ in order to support the theoretical outcomes. In Secs. V and VI, we extend the discussion to the nonminimal combinations, and finally, we summarize the obtained results in the last section.

II. FIELD EQUATIONS OF THE THEORY

In this section, we obtain the field equations of $f(R,T)$ gravity and then introduce some dimensionless variables to simplify the corresponding equations. The action can be written in the form

$$S=\int\sqrt{-g}d^4x\left[\frac{1}{16\pi G}f(R,T^{(\mathrm{m})})+L^{(\mathrm{m})}+L^{(\mathrm{rad})}\right], \quad (2.1)$$

where R is the Ricci scalar, $T^{(\mathrm{m})}\equiv g^{\mu\nu}T^{(\mathrm{m})}_{\mu\nu}$ is the trace of the energy-momentum tensor, the superscript m stands for the dust matter, $f(R,T^{(\mathrm{m})})$ is an arbitrary function of the Ricci scalar and $T^{(\mathrm{m})}$, $L^{(\mathrm{m})}$ and $L^{(\mathrm{rad})}$ are the Lagrangians of the dust matter and radiation, g is the determinant of the metric, and we set $c=1$. As $T^{(\mathrm{rad})}=0$, the trace of the radiation energy-momentum tensor does not play any role in the function of $f(R,T^{(\mathrm{m})})$ and henceforth we drop the superscript m from the trace $T^{(\mathrm{m})}$ unless it is necessary. The energy-momentum tensor is usually defined as the Euler-Lagrange expression of the matter Lagrangian, i.e.,

$$T_{\mu\nu}\equiv-\frac{2}{\sqrt{-g}}\frac{\delta[\sqrt{-g}(L^{(\mathrm{m})}+L^{(\mathrm{rad})})]}{\delta g^{\mu\nu}}, \quad (2.2)$$

and if one assumes that both the Lagrangians depend only on the metric and not on its derivatives, one will get

$$T_{\mu\nu}=g_{\mu\nu}[L^{(\mathrm{m})}+L^{(\mathrm{rad})}]-2\frac{\partial[L^{(\mathrm{m})}+L^{(\mathrm{rad})}]}{\partial g^{\mu\nu}}. \quad (2.3)$$

By the metric variation of the action (2.1), the field equations are[7]

$$F(R,T)R_{\mu\nu}-\frac{1}{2}f(R,T)g_{\mu\nu}+(g_{\mu\nu}\Box-\nabla_\mu\nabla_\nu)F(R,T)=(8\pi G+\mathcal{F}(R,T))T^{(\mathrm{m})}_{\mu\nu}+8\pi GT^{(\mathrm{rad})}_{\mu\nu}, \quad (2.4)$$

where it is helpful to define the derivatives with respect to the trace T and the Ricci scalar R as

$$\mathcal{F}(R,T)\equiv\frac{\partial f(R,T)}{\partial T}\quad\text{and}\quad F(R,T)\equiv\frac{\partial f(R,T)}{\partial R}, \quad (2.5)$$

[7]By the variational (functional) derivative procedure (see, e.g., Refs. [1,77]) and employing the Palatini equation (identity), one can usually derive field equations; nevertheless, one can consult the detailed derivation of these field equations in Ref. [63].

and we have used

$$g^{\alpha\beta}\frac{\delta T^{(\mathrm{m})}_{\alpha\beta}}{\delta g^{\mu\nu}}=-2T^{(\mathrm{m})}_{\mu\nu}. \quad (2.6)$$

Also, by contracting Eq. (2.4), we have

$$F(R,T)R+3\Box F(R,T)-2f(R,T)=(8\pi G+\mathcal{F}(R,T))T. \quad (2.7)$$

Now, in this model, we assume a perfect fluid and a spatially flat Friedmann-Lemaître-Robertson-Walker (FLRW) metric,

$$ds^2=-dt^2+a^2(t)(dx^2+dy^2+dz^2), \quad (2.8)$$

where $a(t)$ is the scale factor. Let us rewrite Eq. (2.4) in a standard form similar to GR, i.e.,

$$G_{\mu\nu}=\frac{8\pi G}{F(R,T)}(T^{(\mathrm{m})}_{\mu\nu}+T^{(\mathrm{rad})}_{\mu\nu}+T^{(\mathrm{eff})}_{\mu\nu}), \quad (2.9)$$

where

$$T^{(\mathrm{eff})}_{\mu\nu}\equiv\frac{1}{8\pi G}\left[\frac{1}{2}(f(R,T)-F(R,T)R)g_{\mu\nu}+(\nabla_\mu\nabla_\nu-g_{\mu\nu}\Box)F(R,T)+\mathcal{F}(R,T)T^{(\mathrm{m})}_{\mu\nu}\right]. \quad (2.10)$$

Regarding the Bianchi identity,[8] obviously in $f(R,T)$ gravity the above effective energy-momentum tensor is not conserved. Thus, by applying the conservation of the energy-momentum tensor of all matter and knowing that $\nabla^\mu T^{(\mathrm{m})}_{\mu\nu}=0=\nabla^\mu T^{(\mathrm{rad})}_{\mu\nu}$, the following constraint must hold:

$$\frac{3}{2}H(t)\mathcal{F}(R,T)=\dot{\mathcal{F}}(R,T), \quad (2.11)$$

where a dot denotes the derivative with respect to the cosmic time t and $H(t)=\dot{a}(t)/a(t)$ is the Hubble parameter. Obviously this relation leads to some restrictions on the functionality of $f(R,T)$, as we shall see in the next section. Equations (2.4) and (2.7), by assuming the metric (2.8), give

$$3H^2F(R,T)+\frac{1}{2}(f(R,T)-F(R,T)R)+3\dot{F}(R,T)H=(8\pi G+\mathcal{F}(R,T))\rho^{(\mathrm{m})}+8\pi G\rho^{(\mathrm{rad})} \quad (2.12)$$

[8]It is well known that the use of the action principle and the principle of general invariance allows one to make immediate connections between symmetry principles and conservation laws, which can be established as inner identities. That is, the metric variation of each Lagrangian density (as a scalar density) of weight one—which is a function of the metric and its derivatives—makes the covariant divergence of the Euler-Lagrange expression of the Lagrangian density identically vanish, e.g., $\nabla^\mu T_{\mu\nu}\equiv 0$; see any text on gravitation, e.g., Ref. [78].

as the Friedmann-like equation, and

$$2F(R,T)\dot{H} + \ddot{F}(R,T) - \dot{F}(R,T)H = -(8\pi G + \mathcal{F}(R,T))\rho^{(\mathrm{m})} - \frac{32}{3}\pi G\rho^{(\mathrm{rad})} \tag{2.13}$$

as the Raychaudhuri-like equation.

In the following, we assume that these functions of $f(R,T)$ can be explicitly written as combinations of a function $g(R)$ and a function $h(T)$, e.g., $f(R,T) = g(R)h(T)$; however, due to the constraint equation (2.11), their forms will be restricted. Now, it is convenient to introduce a few dimensionless independent variables to simplify the obtained equations in the phase space used in the following sections. These variables are defined as

$$x_1 \equiv -\frac{\dot{g}'(R)}{Hg'(R)}, \tag{2.14}$$

$$x_2 \equiv -\frac{g(R)}{6H^2g'(R)}, \tag{2.15}$$

$$x_3 \equiv \frac{R}{6H^2} = \frac{\dot{H}}{H^2} + 2, \tag{2.16}$$

$$x_4 \equiv -\frac{h(T)}{3H^2g'(R)}, \tag{2.17}$$

$$x_5 \equiv \frac{8\pi G\rho^{(\mathrm{rad})}}{3H^2g'(R)}, \tag{2.18}$$

$$x_6 \equiv -\frac{Th'(T)}{3H^2g'(R)}, \tag{2.19}$$

where the prime denotes a derivative with respect to the argument and we have used $R = 6(\dot{H} + 2H^2)$ for the metric (2.8). However, it will be shown in Sec. III that these six variables of the phase space reduce to five independent variables once the constraint equation (2.11) is applied. One may also define some other dimensionless parameters that can play the role of a parametrization in the determination of the function $f(R,T)$, namely,

$$m \equiv \frac{Rg''(R)}{g'(R)}, \tag{2.20}$$

$$r \equiv -\frac{Rg'(R)}{g(R)} = \frac{x_3}{x_2}, \tag{2.21}$$

$$n \equiv \frac{Th''(T)}{h'(T)}, \tag{2.22}$$

$$s \equiv \frac{Th'(T)}{h(T)} = \frac{x_6}{x_4}, \tag{2.23}$$

where $g(R) \neq$ constant and $h(T) \neq$ constant. Note that, generally, we have[9] $m = m(r)$ and $n = n(s)$.

From the Friedmann equations in GR with the FLRW metric, one finds the relation $w = p/\rho = -1 - 2\dot{H}/3H^2$ for the equation of state. Analogously, if one correspondingly defines an effective equation of state (for an effective pressure and an effective energy density) as $w^{(\mathrm{eff})} = p^{(\mathrm{eff})}/\rho^{(\mathrm{eff})} \equiv -1 - 2\dot{H}/3H^2$, then one will obtain the effective equation of state as follows. First, to facilitate matching with SNIa observations, let us redefine Eqs. (2.12) and (2.13) as

$$3AH^2 = 8\pi G(\rho^{(\mathrm{m})} + \rho^{(\mathrm{rad})} + \rho^{(\mathrm{DE})}) \tag{2.24}$$

and

$$-2A\dot{H} = 8\pi G(\rho^{(\mathrm{m})} + (4/3)\rho^{(\mathrm{rad})} + \rho^{(\mathrm{DE})} + p^{(\mathrm{DE})}), \tag{2.25}$$

where A is a constant and $\rho^{(\mathrm{DE})}$ and $p^{(\mathrm{DE})}$ denote the density and the pressure of the dark energy, respectively, defined as

$$8\pi G\rho^{(\mathrm{DE})} \equiv \mathcal{F}\rho^{(\mathrm{m})} - 3\dot{F}(R,T)H - \frac{1}{2}(f(R,T) - F(R,T)R) + 3H^2(A - F) \tag{2.26}$$

and

$$8\pi Gp^{(\mathrm{DE})} \equiv \ddot{F}(R,T) + 2\dot{F}(R,T)H + \frac{1}{2}(f(R,T) - F(R,T)R) - (2\dot{H} + 3H^2)(A - F). \tag{2.27}$$

Thus, the equation of state parameter for the dark energy is given as $w^{(\mathrm{DE})} \equiv p^{(\mathrm{DE})}/\rho^{(\mathrm{DE})}$.

The definitions (2.26) and (2.27) lead to the continuity equation for the dark energy component, namely,

$$\dot{\rho}^{(\mathrm{DE})} + 3H(\rho^{(\mathrm{DE})} + p^{(\mathrm{DE})}) = 0. \tag{2.28}$$

Now, we can rewrite the effective equation of state in the following form:

$$w^{(\mathrm{eff})} = \frac{F}{A}\left(\Omega^{(\mathrm{DE})}w^{(\mathrm{DE})} + \frac{\Omega^{(\mathrm{rad})}}{3}\right), \tag{2.29}$$

where we have defined

$$\Omega^{(\mathrm{rad})} \equiv \frac{8\pi G\rho^{(\mathrm{rad})}}{3H^2F} \quad \text{and} \quad \Omega^{(\mathrm{DE})} \equiv \frac{8\pi G\rho^{(\mathrm{DE})}}{3H^2F}, \tag{2.30}$$

which lead to the usual density parameters for GR. Using the definition (2.16), in a suitable form $w^{(\mathrm{eff})}$ reads

[9] Actually, in principle one can derive R and T from Eqs. (2.21) and (2.23) in terms of r and s, respectively. Hence, one gets $m = m(r)$ and $n = n(s)$.

$$w^{(\mathrm{eff})} = \frac{1}{3}(1 - 2x_3). \tag{2.31}$$

Also, for general matter, the cosmological solutions for a constant value of x_3 are [using Eq. (2.16)]

$$a(t) = a_0\left(\frac{t - t_i}{t_0 - t_i}\right)^{\frac{1}{2-x_3}}, \tag{2.32}$$

and for the conservation of the energy-momentum tensor one has

$$\dot{\rho}(t) + 2(2 - x_3)H(t)\rho(t) = 0, \tag{2.33}$$

where a_0 and t_0 are the integral constants that can be fixed by the present values, and for t_i we set $a(t_i) = 0$. Equations (2.32) and (2.33) hold for all values of x_3 except for $x_3 = 2$. In this special case we have $\dot{H} = 0$, which leads to either a de Sitter solution or a static one.

In the next section, we consider a particular form of the function $f(R,T)$ and show that the acceptable solution trajectories tend to transit from the radiation era with $x_3 = 0$ to the dust-like matter era with $x_3 = 1/2$, where, for these two values, the conservation equation (2.33) gives,[10] respectively,

$$\dot{\rho}^{(\mathrm{rad})} + 4H\rho^{(\mathrm{rad})} = 0 \tag{2.34}$$

and

$$\dot{\rho}^{(m)} + 3H\rho^{(m)} = 0. \tag{2.35}$$

III. DYNAMICAL SYSTEMS APPROACH OF THE MINIMAL CASE $f(R,T) = g(R) + h(T)$

In this section, we investigate the model by employing the dynamical systems approach. First we consider the case when the geometrical sector and the matter sector in the function $f(R,T)$ are minimally coupled.[11] The case of nonminimal coupling is considered in later sections. In the minimal case, we assume that the form of function $f(R,T)$ is

$$f(R,T) = g(R) + h(T), \tag{3.1}$$

where $h(T)$ and $g(R)$ are arbitrary functions and hereafter we show the functions $g(R)$, $h(T)$ and their derivatives without indicating their arguments for the sake of convenience.

The dynamical systems approach[12] introduces a relatively simple technique to investigate the whole space of solutions in the form of some extremum points (the fixed points), by which the evolution of the system can be pictured qualitatively near these points. A qualitative study is possible via checking the phase-space trajectories, whose behaviors are sensitive to initial conditions. In this way, one can obtain different descriptions dependent on different initial conditions and which therefore indicate the initial conditions that lead to a desired physical result. In cosmological applications, one is capable of determining the early- and late-time behaviors of models with this technique (in addition to possible matter or radiation solutions). That is, one can achieve a global picture of all solutions and behaviors of the system near these solutions. As a result, through the dynamical systems approach, the inconsistent models can be ruled out, and those models which deserve further investigation could be selected. For a recent application of the dynamical systems approach to some modified theories of gravity see, e.g., Refs. [80–82].

Now, rewriting Eqs. (2.12) and (2.13) with (3.1) gives

$$1 + \frac{g}{6H^2g'} + \frac{h}{6H^2g'} - \frac{R}{6H^2} + \frac{\dot{g}'}{Hg'} = \frac{8\pi G\rho^{(\mathrm{m})}}{3H^2g'} + \frac{h'\rho^{(\mathrm{m})}}{3H^2g'} + \frac{8\pi G\rho^{(\mathrm{rad})}}{3H^2g'} \tag{3.2}$$

and

$$2\frac{\dot{H}}{H^2} + \frac{\ddot{g}'}{H^2g'} - \frac{\dot{g}'}{Hg'} = -\frac{8\pi G\rho^{(\mathrm{m})}}{H^2g'} - \frac{h'\rho^{(\mathrm{m})}}{H^2g'} - \frac{32\pi G\rho^{(\mathrm{rad})}}{3H^2g'}. \tag{3.3}$$

In the dynamical systems approach, the original EOM [e.g., Eqs. (3.2) and (3.3) in this work] can be cast in the form of some new evolutionary EOM in terms of new variables (which are constructed from the original ones) and their first derivatives. Then, the solutions of these new EOM are indicated as some fixed points of the system which are obtained through an extremization, where if the new EOM do not explicitly contain time then the system will be called an autonomous one. We employ this approach to extract and analyze the solutions of Eqs. (3.2) and (3.3) by employing the introduced variables (2.14)–(2.23).

First of all, the constraint (2.11) for the minimal case with $h \neq$ constant gives

$$Th'' = -\frac{1}{2}h', \tag{3.4}$$

i.e., by Eq. (2.22), $n = -1/2$, and by integrating with respect to the trace T, this reads

$$Th' - \frac{1}{2}h + C = 0, \tag{3.5}$$

where C is an integration constant. This constant must be zero to be consistent with condition (3.16), as we will show. Thus, Eq. (3.5) with $C = 0$ leads to $s = 1/2$, and hence the relation $x_6 = x_4/2$. Therefore, with these unique constants n and s the phase-space variables of the model are reduced

[10] Analogously, the radiation and dust-like types of matter are dictated from the appearance of the corresponding equations.

[11] We apply the conventional terminology used in the literature for adding and crossing two terms in the Lagrangian as the minimal and the nonminimal couplings, respectively.

[12] See Ref. [79] and references therein.

from six to five. As we will see, this reduction makes the problem more tractable.

Obviously, all cases with $x_4 = 0$ [for a nonsingular denominator in Eq. (2.17)] in the minimal case get returned to $f(R)$ gravity; however, the cases with a nonzero x_4 give more general solutions than $f(R)$ gravity. Also, all cases with $h =$ constant can be considered in an $f(R)$ gravity background and act as if they have a cosmological constant. Here, by applying Eq. (3.4), the only form that respects the conservation law in the minimal case is

$$f(R, T) = g(R) + c_1\sqrt{-T} + c_2, \tag{3.6}$$

where c_1 and c_2 are some constants with respect to T; however, in general they can be functions of the Ricci scalar R. Those cases in which c_1 is a function of R will be considered as nonminimal in the subsequent section. Now, let us obtain the possible "good" cosmological solutions, i.e., those solutions that describe a dust-like matter-dominated era followed by an accelerated era for the general case (3.6).

Equation (3.2) gives a constraint for the defined variables (2.14)–(2.18),

$$\Omega^{(\mathrm{m})} \equiv \frac{8\pi G\rho^{(\mathrm{m})}}{3H^2 g'} = 1 - x_1 - x_2 - x_3 - x_4 - x_5. \tag{3.7}$$

Hence, the autonomous EOM for the five independent variables (2.14)–(2.18) can be achieved via

$$\frac{dx_1}{dN} = -1 + x_1(x_1 - x_3) - 3x_2 - x_3 - \frac{3}{2}x_4 + x_5, \tag{3.8}$$

$$\frac{dx_2}{dN} = \frac{x_1 x_3}{m} + x_2(4 + x_1 - 2x_3), \tag{3.9}$$

$$\frac{dx_3}{dN} = -\frac{x_1 x_3}{m} + 2x_3(2 - x_3), \tag{3.10}$$

$$\frac{dx_4}{dN} = x_4\left(\frac{5}{2} + x_1 - 2x_3\right), \tag{3.11}$$

$$\frac{dx_5}{dN} = x_5(x_1 - 2x_3), \tag{3.12}$$

where N represents a derivative with respect to $\ln a$ and Eq. (3.7) has been used. The solutions for the system of equations (3.8)–(3.12) for arbitrary $m(r)$, $n(s) = -1/2$, and $s = 1/2$ are listed in Table I. These solutions include ten fixed points P_1–P_{10} at which the variables x_1–x_5 (and any arbitrary function of them) take their critical values, i.e., these are solutions to the system of equations $dx_i/dN = 0$, $i = 1, \ldots, 5$. Thus, in general the parameters $r = r(x_2, x_3)$ and $s = s(x_4, x_6)$ must take their critical values too. That is,

$$\frac{dr}{dN} = \frac{\partial r(x_2, x_3)}{\partial x_2}\frac{dx_2}{dN} + \frac{\partial r(x_2, x_3)}{\partial x_3}\frac{dx_3}{dN} = 0 \tag{3.13}$$

and

$$\frac{ds}{dN} = \frac{\partial s(x_4, x_6)}{\partial x_4}\frac{dx_4}{dN} + \frac{\partial s(x_4, x_6)}{\partial x_6}\frac{dx_6}{dN} = 0, \tag{3.14}$$

which, using definitions (2.15)–(2.17), (2.19)–(2.21), and (2.23), give

$$0 = \frac{dr}{dN} = -r\left(\frac{1 + r + m(r)}{m(r)}\right)x_1 \equiv -r\mathcal{M}(r)x_1 \tag{3.15}$$

and

$$0 = \frac{ds}{dN} = 3s(s - n(s) - 1), \tag{3.16}$$

where we have defined

$$\mathcal{M}(r) \equiv \frac{1 + r + m(r)}{m(r)}, \tag{3.17}$$

TABLE I. The fixed-point solutions of the dynamical systems approach of $f(R, T) = g(R) + h(T)$.

Fixed point	Coordinates $(x_1, x_2, x_3, x_4, x_5)$	Scale factor	$\Omega^{(\mathrm{m})}$	$\Omega^{(\mathrm{rad})}$	$w^{(\mathrm{eff})}$
P_1	$\left(\frac{3m}{2(1+m)}, -\frac{5+8m}{4(1+m)^2}, \frac{5+8m}{4(1+m)}, \frac{4-m(3+10m)}{4(1+m)^2}, 0\right)$	$a(t) = a_0(\frac{t-t_i}{t_0-t_i})^{\frac{4(1+m)}{3}}$	0	0	$-\frac{1+2m}{2(1+m)}$
P_2	$\left(\frac{2(1-m)}{1+2m}, \frac{1-4m}{m(1+2m)}, -\frac{(1-4m)(1+m)}{m(1+2m)}, 0, 0\right)$	$a(t) = a_0(\frac{t-t_i}{t_0-t_i})^{\frac{m(1+2m)}{1-m}}$	0	0	$\frac{2-5m-6m^2}{3m(1+2m)}$
P_3	$\left(\frac{3m}{1+m}, -\frac{1+4m}{2(1+m)^2}, \frac{1+4m}{2(1+m)}, 0, 0\right)$	$a(t) = a_0(\frac{t-t_i}{t_0-t_i})^{\frac{2(1+m)}{3}}$	$\frac{2-m(3+8m)}{2(1+m)^2}$	0	$-\frac{m}{1+m}$
P_4	$(-4, 5, 0, 0, 0)$	$a(t) = a_0(\frac{t-t_i}{t_0-t_i})^{\frac{1}{2}}$	0	0	$\frac{1}{3}$
P_5	$(-\frac{5}{2}, 0, 0, \frac{7}{2}, 0)$	$a(t) = a_0(\frac{t-t_i}{t_0-t_i})^{\frac{1}{2}}$	0	0	$\frac{1}{3}$
P_6	$(-1, 0, 0, 0, 0)$	$a(t) = a_0(\frac{t-t_i}{t_0-t_i})^{\frac{1}{2}}$	2	0	$\frac{1}{3}$
P_7	$(1, 0, 0, 0, 0)$	$a(t) = a_0(\frac{t-t_i}{t_0-t_i})^{\frac{1}{2}}$	0	0	$\frac{1}{3}$
P_8[a]	(0, —1, 2, 0, 0)	$a(t) = a_0 \exp H_0 t$	0	0	-1
P_9	$(0, 0, 0, 0, 1)$	$a(t) = a_0(\frac{t-t_i}{t_0-t_i})^{\frac{1}{2}}$	0	1	$\frac{1}{3}$
P_{10}	$\left(\frac{4m}{1+4m}, -\frac{2m}{(1+m)^2}, \frac{2m}{1+m}, 0, \frac{1-m(2+5m)}{(1+m)^2}\right)$	$a(t) = a_0(\frac{t-t_i}{t_0-t_i})^{\frac{1+m}{2}}$	0	$\frac{1-m(2+5m)}{(1+m)^2}$	$\frac{1-3m}{3(1+m)}$

[a]This solution has $\dot{H} = 0$.

which is well defined for $m(r) \neq 0$.[13] As a result, the condition $ds/dN = 0$ for $s \neq 0$,[14] with $n = -1/2$, leads to $s = 1/2$, which in turn gives a zero value for the constant C in Eq. (3.5). The acceptable solutions are those that respect these two conditions, $dr/dN = 0$ and $ds/dN = 0$. Now, restoring constraint (2.11), from Eqs. (3.15) and (3.16) it turns out that all acceptable solutions must lie in one of the following three categories:

$$\begin{cases} 1)\ r = 0, & s = \frac{1}{2} = -n, \\ 2)\ \mathcal{M}(r) = 0, & s = \frac{1}{2} = -n, \\ 3)\ x_1 = 0, & s = \frac{1}{2} = -n. \end{cases} \tag{3.18}$$

A glance at Table I shows that the points P_1, P_2, P_3, and P_{10} satisfy the condition $m(r) = -r - 1$, the parameter r vanishes for the point P_4, and for the points P_8 and P_9 we have $x_1 = 0$. These are the only obvious points that respect Eq. (3.18). The other points have both $x_2 = 0$ and $x_3 = 0$, which clearly implies that there is an ambiguity in determining r. Nevertheless, these points actually do satisfy Eqs. (3.15) and (3.16), and hence r can be determined by a straightforward calculation using definition (2.21). In this respect, we assume that the condition $m(r) = -r - 1$ should be valid for all of the points, and use it wherever it is necessary.

In the following discussions, the stability analysis of the fixed points are performed via inspecting their corresponding eigenvalues. Imprecisely speaking, the trajectories of the phase space advance to a fixed point if all eigenvalues have negative values, and recede from a fixed point if all eigenvalues have positive values. In this respect, the fixed points occurring in the former and the latter sets are called the stable and unstable points, respectively. The fixed points with both positive and negative eigenvalues are called saddle points, and those trajectories which advance to a saddle fixed point along some eigenvectors may recede from it along some other eigenvectors.

In Sec. III A, we investigate the properties of each of the fixed points of Table I in the absence of the radiation. Since the calculations in a system with five degrees of freedom can be very messy and time-consuming, we consider the effects of the radiation in Sec. III B. Also, in Sec. III C, we illustrate "good" cosmological solutions, i.e., those solutions that determine the trajectories which connect the dust-matter-dominated points to the accelerated-expansion-dominated points. Incidentally, the considerations have been assisted by numerical manipulations wherever the exact computations have not been possible.

[13]Note that all solutions that satisfy $m(r) = -r - 1$ must satisfy $\mathcal{M}(r) = 0$ as a more strong constraint; this fact affects the analysis involved in Sec. IV.

[14]Note that the corresponding solutions with $s = 0$ have been discarded, for they contradict the former result $n = -1/2$.

A. Properties of fixed points in the absence of radiation

In the absence of radiation, there are only the first eight fixed points P_1–P_8. While presenting the properties of these points, we compare the results with the corresponding results of $f(R)$ gravity in Ref. [76] (whenever it is necessary), and briefly indicate the obtained results in Table II.

(i) P_1

This is a new fixed point which corresponds to a curvature-dominated point.[15] This point can play the role of an accelerated-expansion point provided that $w^{(\mathrm{eff})} < -1/3$ for $m > -1/4$ and $m < -1$. In the former range, we have a nonphantom accelerated universe, and the latter one lies in a phantom domain. The eigenvalues of this point are obtained as

$$-\frac{3}{2}, \quad -\frac{3m(1+m)(3+2m) + a(m)}{8m(1+m)^2}, \quad \frac{-3m(1+m)(3+2m) + a(m)}{8m(1+m)^2}, \quad \frac{3}{2}(1+m'), \tag{3.19}$$

where

$$a(m) \equiv \{m(1+m)^2 \times [-160 + m(-55 + 700m + 676m^2)]\}^{1/2}, \tag{3.20}$$

and $m' \equiv dm/dr$. The above eigenvalues show that with $m' > -1$, we have a saddle point. However, for $m' < -1$, the point P_1 is a stable point when $-4/5 < m < -5/8$ or $0.43 < m < 1/2$ with real-valued eigenvalues, a spiral stable point when $0 < m \leq 0.43$, and a saddle point otherwise. Nevertheless, within these ranges the first one does not lead to the condition $w^{(\mathrm{eff})} < -1/3$, and hence we discard it. As a result, the point P_1 introduces two new ranges that can accelerate the universe in the nonphantom domain, which collectively are

$$m' < -1, \qquad 0 < m < \frac{1}{2}, \qquad -\frac{2}{3} < w^{(\mathrm{eff})} < -\frac{1}{2}. \tag{3.21}$$

In the limit $|\, m \,| \longmapsto 0$, the eigenvalues are

$$-\frac{3}{2}, \quad -\frac{9}{8} + \sqrt{-\frac{5}{2m}}, \quad -\frac{9}{8} - \sqrt{-\frac{5}{2m}}, \quad \frac{3}{2}(1+m'). \tag{3.22}$$

[15]We refer to a point with both properties $\Omega^{(\mathrm{m})} = 0 = \Omega^{(\mathrm{rad})}$ as a curvature-dominated point.

TABLE II. The stability of the fixed points in both $f(R,T)$ and $f(R)$ gravities without radiation.

Fixed point	Stability in $f(R,T)$ gravity	Stability in $f(R)$ gravity
P_1	$\begin{cases} a)\ \forall\ m, m' > -1$, saddle $b)\ 0 < m < 1/2, m' < -1$, stable $c)\ m \to \pm\infty, \forall\ m'$, saddle \end{cases}$	Does not appear
P_2	$\begin{cases} d)\ 0 < m < 1/4, m' > -1$, unstable $e)\ m < -1/2(1+\sqrt{3}), m' > -1$, stable $f)\ -1/2 < m < 0, m' > -1$, stable $g)\ m > 1, m' > -1$, stable $h)\ 1/2 < m < 1, m' < -1$, stable $i)\ m \to \pm\infty, m' > -1$, stable \end{cases}$	$\begin{cases} \text{The same properties except for} \\ h)\ (1/2)(-1+\sqrt{3}) < m < 1, m' < -1$, stable \end{cases}$
P_3	Always a saddle point	$\begin{cases} j)\ 0 < m < 0.327, m' > -1$, saddle $k)\ \forall\ m, m' = 0$, saddle \end{cases}$
P_4	$\begin{cases} l)\ -1 < m < 0$, stable; otherwise saddle $m)\ P_4 = P_{2\|m=-1} \end{cases}$	The same properties
P_5	$\begin{cases} n)\ \forall\ m, m' = 0$, saddle; otherwise saddle or stable $o)\ m \to 0^-, m' < 0$, stable; otherwise saddle \end{cases}$	Does not appear
P_6	Always a saddle point	$p)\ \forall\ m, m' = 0$, saddle; otherwise saddle or stable
P_7	$\begin{cases} q)\ \forall\ m, m' \neq 0$, saddle or unstable $r)\ 0 < m < 1/4, m' = 0$, saddle; otherwise stable $s)\ m \to 0^-, m' < 0$, unstable; otherwisesaddle $t)\ P_7 = P_{2\|m=1/4} \end{cases}$	The same properties
P_8	$\begin{cases} u)\ 0 < m < 16/25, r = -2$, spiral stable $v)\ 16/25 \leq m < 1, r = -2$, stable $w)$ Otherwise saddle \end{cases}$	The same properties

This means that, for $m \to 0^+$, this point is a spiral stable point when $m' < -1$ and a saddle point otherwise. When $\mid m \mid \to \infty$, the point tends to a de Sitter point with coordinates $(3/2, 0, 2, -5/2)$, which is not a stable point. Indeed, from Eq. (3.19) it is obvious that P_1 is a permanent saddle point in both of the limits $m' = 0$ and $\mid m \mid \to \infty$.

(ii) P_2

The point P_2 also has $\Omega^{(\mathrm{m})} = 0 = \Omega^{(\mathrm{rad})}$, and like P_1 is a curvature-dominated point whose effective equation of state depends on the parameter m. An accelerated-expansion behavior can be achieved when $m < (-1-\sqrt{3})/2$ or $(-1+\sqrt{3})/2 < m < 1$ in the nonphantom domain, and when $-1/2 < m < 0$ or $m > 1$ in the phantom domain. The eigenvalues are obtained as

$$-4+\frac{1}{m}, \qquad \frac{-8m^2-3m+2}{m(1+2m)}, \qquad \frac{2(1-m^2)(1+m')}{m(1+2m)}, \qquad \frac{-10m^2-3m+4}{2m(1+2m)}. \tag{3.23}$$

In the limit $\mid m \mid \to \infty$, it asymptotically reaches the point $P_{2,\mathrm{dS}} = (-1, 0, 2, 0)$—at which the universe expands as a de Sitter accelerated one—and is a stable point for $m' > -1$. In the opposite limit, when $\mid m \mid \to 0$, the eigenvalues are

$$\frac{1}{m}, \qquad \frac{2}{m}, \qquad \frac{2}{m}(1+m'), \qquad \frac{2}{m}.$$

Thus, in order to have a stable acceleration era one must have $m \to 0^-$ and $m' > -1$ simultaneously. An investigation of the eigenvalues gives ranges of m in which one can expect a stable accelerated-expansion behavior. For the nonphantom domain, we have

$$\mathcal{A})\ m' > -1, \quad m < -\frac{1}{2}(1+\sqrt{3}), \quad -1 < w^{(\mathrm{eff})} < -\frac{1}{3}, \tag{3.24}$$

$$\mathcal{B})\ m' < -1, \qquad \frac{1}{2} < m < 1, \qquad -1 < w^{(\mathrm{eff})} < -\frac{2}{3}, \tag{3.25}$$

and for the phantom domain we have

$$\mathcal{C})\ m' > -1, \qquad m > 1, \qquad -1.07 < w^{(\mathrm{eff})} < -1, \tag{3.26}$$

$$\mathcal{D})\ m' > -1, \qquad -\frac{1}{2} < m < 0, \qquad w^{(\mathrm{eff})} < -7.60. \tag{3.27}$$

However, P_2 is an unstable point in the range $0 < m < 1/4$ provided that $m' > -1$. The properties of this point do not change in this model compared to $f(R)$ gravity, except in the case $\mathcal{B}$, where the range m becomes more restricted, i.e., the corresponding range is $(\sqrt{3}-1)/2 < m < 1$ in the case $\mathcal{B}$ in $f(R)$ gravity.

(iii) P_3

The point through which we can search for a matter era is P_3, which also appears in $f(R)$ gravity. For $m = 0$, we have $w^{(\mathrm{eff})} = 0$ and $\Omega^{(\mathrm{m})} = 1$. The eigenvalues are

$$\frac{3}{2}, \quad \frac{-3m + b(m)}{4m(1+m)}, \quad \frac{-3m - b(m)}{4m(1+m)}, \quad 3(1+m'), \tag{3.28}$$

where

$$b(m) \equiv [m(256m^3 + 160m^2 - 31m - 16)]^{1/2}. \tag{3.29}$$

The existence of the positive constant eigenvalue $3/2$ means that the point P_3 is not stable; instead, it is always a saddle point. It is an interesting result that does not occur in $f(R)$ gravity. For infinitesimal values of the parameter m, we can approximate the eigenvalues as

$$\frac{3}{2}, \quad -\frac{3}{4} + \sqrt{-\frac{1}{m}}, \quad -\frac{3}{4} - \sqrt{-\frac{1}{m}}, \quad 3(1+m'). \tag{3.30}$$

In the limit $m \to 0^+$, we have an acceptable saddle-point matter era. However, the point P_3 in the limit $m \to 0^-$ is not generally acceptable, for the second eigenvalue takes a large positive real value. Therefore, the matter era becomes very short, so that the observational data cannot be matched. The point P_3 contains some ranges in which the universe can be accelerated but not in a usual way, for the accelerating conditions are

$$\mathcal{E})\ m > \frac{1}{2}, \quad -1 < w^{(\mathrm{eff})} < -\frac{1}{3}, \quad -4 < \Omega^{(m)} < -\frac{1}{3}, \tag{3.31}$$

$$\mathcal{F})\ m < -1, \quad w^{(\mathrm{eff})} < -1, \quad \Omega^{(m)} < -4. \tag{3.32}$$

That is, the accelerated expansion can occur with a negative value for the matter-density parameter, which is not physically interesting. Considering the definition used in Eq. (3.7), the solutions denoting $\Omega^{(\mathrm{m})} < 0$ are ruled out in the background of viable $f(R)$ models with the condition[16] $g'(R) > 0$, which we have also adopted here.

(iv) P_4, P_5, and P_7

There are three points in $f(R,T)$ gravity with $\Omega^{(\mathrm{m})} = 0$ and $\Omega^{(\mathrm{rad})} = 0$ whose equations of state mimic the one for radiation. As these points do not correspond to any known matter, they are not physically interesting. Hence, we discard these solutions in Sec. III C as nonphysical ones.

The point P_4 is a special case of P_2 if m is set to be $m = -1$, and its eigenvalues are found to be

$$-5, \quad -3, \quad 4\left(1 + \frac{1}{m}\right), \quad -\frac{3}{2}. \tag{3.33}$$

When $-1 < m < 0$, the point P_4 is a stable point, and is a saddle point otherwise. This property has the same features in $f(R)$ gravity.

The point P_5 is a new solution, which does not appear in $f(R)$ gravity. The eigenvalues are

$$-\frac{7}{2}, \quad -\frac{3}{2}, \quad \frac{m(5+11m) - 5r(1+r)m' - 5c(m,m')}{4m^2}, \quad \frac{m(5+11m) - 5r(1+r)m' + 5c(m,m')}{4m^2}, \tag{3.34}$$

where

$$c(m,m') \equiv \{m^2(1+m)^2 + rm'[-2m(1+m) + 2(-1+m)mr + r(1+r)^2 m']\}^{1/2}. \tag{3.35}$$

As it is obvious the point P_5 never becomes unstable. When m is a nonzero constant, we have the eigenvalues

$$-\frac{7}{2}, \quad -\frac{3}{2}, \quad \frac{3}{2}, \quad 4 + \frac{5}{2m}, \tag{3.36}$$

i.e., P_5 is a saddle point for constant m. When $m \to 0$, the eigenvalues become

$$-\frac{7}{2}, \quad -\frac{3}{2}, \quad -\frac{5m'}{2m}, \quad \frac{5}{2m}. \tag{3.37}$$

Therefore, when $m \to 0^-$ with $m' < 0$, this point is stable, and otherwise it is a saddle point.

The last point in this category is P_7, which is regarded as a special case of the point P_2 for $m = 1/4$. This point has eigenvalues

[16] This condition guaranties that the gravity force is an attractive one. Hence, as $f(R)$ theories are special cases with $h(T) = 0$ in the minimal coupling case, this condition should hold.

$$\frac{7}{2}, \quad 2, \quad \frac{m(-1+9m)+r(1+r)m'-c(m,m')}{2m^2}, \quad \frac{m(-1+9m)+r(1+r)m'+c(m,m')}{2m^2}. \tag{3.38}$$

Thus P_7 cannot be a stable point. When m is a nonzero constant, the eigenvalues (3.38) read

$$\frac{7}{2}, \quad 2, \quad 4-\frac{1}{m}, \quad 5, \tag{3.39}$$

i.e., for $0 < m < 1/4$ the point P_7 is a saddle point, and otherwise it behaves as an unstable point. In the limit $m \to 0$, the eigenvalues behave as

$$\frac{7}{2}, \quad 2, \quad -\frac{1}{m}, \quad \frac{m'}{m}, \tag{3.40}$$

where for $m \to 0^-$ and $m' < 0$ this point is unstable, and otherwise it is a saddle point.

(v) P_6

This is a point with an unusual feature. The value of the density parameter $\Omega^{(m)}$ does not match the equation of state in a meaningful manner, for we have $w^{(\text{eff})} = 1/3$ and $\Omega^{(m)} = 2$. However, in this model it may occur that the universe approaches this point. Hence, like the points P_4, P_5, and P_7, the stability of this point should be considered. The eigenvalues are given by

$$-2, \quad \frac{3}{2}, \quad \frac{m(1+7m)-r(1+r)m'-c(m,m')}{2m^2}, \quad \frac{m(1+7m)-r(1+r)m'+c(m,m')}{2m^2}. \tag{3.41}$$

The first two eigenvalues, -2 and $3/2$, show that this point is always a saddle point for all values of m and m'.

(vi) P_8

The point P_8 is the only de Sitter fixed point of the minimally coupled form of $f(R,T)$ gravity. The corresponding eigenvalues are represented as

$$-3, \quad -\frac{3}{2}, \quad \frac{1}{2}\left(-3-\sqrt{25-\frac{16}{m}}\right), \quad \frac{1}{2}\left(-3+\sqrt{25-\frac{16}{m}}\right). \tag{3.42}$$

This point is a stable one in the range $0 < m < 1$, and otherwise it is a saddle point.

B. Effects of radiation

In this subsection, we take into account the effects of radiation for the fixed points, and in particular we check any possible change in the stability of the fixed points[17] P_1, P_2, P_3, and P_8.

The existence of radiation adds two new fixed points P_9 and P_{10}, as shown in Table I. The point P_9 is a standard radiation point with the eigenvalues (4, 4, 5/2, −1, 1), which denotes that this point is always a saddle point, the same as in $f(R)$ gravity.

The eigenvalues of P_{10} are given as

$$\frac{5}{2}, \quad 1, \quad \frac{m-1+\sqrt{81m^2+30m-15}}{2(m+1)}, \quad \frac{m-1-\sqrt{81m^2+30m-15}}{2(m+1)}, \quad 4(1+m'). \tag{3.43}$$

It is interesting that the point P_{10} is always a saddle point irrespective of the values of m and m', for, numerically, it is impossible for the third and forth eigenvalues to simultaneously take positive values. Furthermore, P_{10}, in the limit $m \to 0$, gives another radiation fixed point in which the eigenvalues are nonsingular, i.e., they are given as

$$\frac{5}{2}, \quad 1, \quad \frac{-1+i\sqrt{15}}{2}, \quad \frac{-1-i\sqrt{15}}{2}, \quad 4(1+m'), \tag{3.44}$$

where m' must be evaluated at $r \to -1$.

The inclusion of radiation does not change the stability properties of the eigenvalues of the other fixed points. In fact, the addition of radiation to the action leads to the appearance of the values $-5/2$, $(2-4m-10m^2)/[m(1+2m)]$, -1, and -4 as the fifth eigenvalues of P_1, P_2, P_3, and P_8, respectively. Thus, it is obvious that none of the stability properties of the accelerated fixed points and the matter point P_3 change. This means that all the cosmological solutions which have a true sequence $P_3 \to P_{1,2,8}$ can include a saddle radiation era for $m \to 0^+$.

C. Cosmological solutions

"Good" cosmological solutions are those that pass a long enough matter-dominated era followed by an accelerated expansion; hence, any matter point contained in the model must be a saddle point in the phase space. However, the eras that show an accelerated expansion should be attractors (stable points) in the phase space. In this study, the only point that involves a matter point is P_3 for $|m| \to 0^+$, and P_1, P_2, P_3, and P_8 can be the accelerated points. Hereafter, we indicate the matter point P_3 with the condition $m(r \approx -1) \to 0$ as $P_3^{(0)}$. It is worth mentioning that any well-defined curve $m(r)$ of each model must satisfy the relations $m(r_i) = -r_i - 1$ and $\mathcal{M}(r_i) = 0$ for some root r_i; the second condition is equal to the first one for cases

[17] As discussed before, the points P_4–P_7 do not have a physical meaning and hence we do not consider them in this subsection.

containing $m(r_i) \neq 0$. The equation $m(r_i) = -r_i - 1$ gives some roots that belong to the points P_1, P_2, or P_3 which we generally indicate as $P_{1(a,b,...)}$, $P_{2(a,b,...)}$, or $P_{3(a,b,...)}$.

The accelerating roots of P_3 labeled by $a, b, \ldots$ correspond to some negative matter-density parameters—such as those shown in Sec. III A—which cannot be physical, and hence we discard them. Consequently, we should consider the cosmological transitions of $P_3^{(0)}$ to either P_1, P_2, or P_8. Another assumption that we apply in the rest of this work is to discard solutions with $m \to 0^-$, for from Eq. (3.30) it is obvious that one of the eigenvalues gets a large positive value for a small negative value of m and hence it diverges for infinitesimal negative values. This means that the trajectories leave the matter era very fast and hence the matter era becomes very short, which causes difficulties in matching the model with observations. Thus, in general, the models with $m \to 0^-$ are unacceptable. We indicate in the following classification that, as P_3 is a saddle point irrespective of the values of m and m', there are more cosmological solutions than in $f(R)$ gravity. We study these transitions in turn, and we suppose that there are some roots in all important regions for the generality of the discussion. Also, we assume that the condition $m(r_i) = -r_i - 1$ holds with $m(r_i) \neq 0$.

(i) $P_3(m'_3 > -1, m > 0)$ and $P_3(m'_3 < -1, m > 0)$ to $P_1(m'_1 < -1, m > 0)$.[18]
The point P_1 is a stable one in the range $0 < m < 1/2$ provided that $m'_1 < -1$, whilst P_3 is always a saddle point. The curve $m(r)$ must intersect[19] the line $m = -r - 1$ with a derivative $m'_3 > -1$ or $m'_3 < -1$ for leaving the matter epoch, and with $m'_1 < -1$ for entering the accelerated epoch. Theoretically, the transition $P_3(m'_3 > -1, m > 0)$ to $P_1(m'_1 < -1, m > 0)$ is possible, as is shown in Fig. 1 (labeled Class I solutions). However, the transition from $P_3(m'_3 < -1, m > 0)$ to $P_1(m'_1 < -1, m > 0)$ is not possible; these solutions are labeled as Class VII$_a$ in Fig. 2. Nevertheless, there is a special case, namely, when P_3 and P_1 are solutions of the model with the same root r, in which one has $m'_{1,3} < -1$. Hence, this demonstrates an acceptable cosmological solution, and we indicate this type of solution as Class II (Fig. 1).

(ii) $P_3(m'_3 > -1, m > 0)$ to $P_2(m'_2 > -1)$ in Regions $\mathcal{A}$, $\mathcal{D}$, $\mathcal{C}$ and to $P_2(m'_2 < -1)$ in Region $\mathcal{B}$.
This class includes two classes of solutions. In the first class, there is no connection between $P_3^{(0)}$ and P_2 in the regions $\mathcal{A}$, $\mathcal{D}$, and $\mathcal{C}$, which we call Class VII$_b$ in Fig. 2. All solutions with either an improper transition (transition from unallowable regions) or without a connection with the matter point $P_3^{(0)}$ fall into this class. In the second class, it is possible to connect $P_3^{(0)}$ with $m'_3 > -1$ to P_2 with $m'_2 < -1$ in the region $\mathcal{B}$; an example of these solutions is labeled as Class III in Fig. 1. Note that these classes of solutions also appear in $f(R)$ gravity.

(iii) $P_3(m'_3 < -1, m > 0)$ to $P_2(m'_2 > -1)$ in Regions $\mathcal{A}$, $\mathcal{D}$, $\mathcal{C}$ and to $P_2(m'_2 < -1)$ in Region $\mathcal{B}$.
Since P_3 is a saddle point irrespective of the value of m', it can be connected to the point P_2 in the regions $\mathcal{A}$, $\mathcal{D}$, and $\mathcal{C}$, the solutions of which are labelled as Class IV in Fig. 1. On the other hand, because we have $m'_{2,3} < -1$ in the region $\mathcal{B}$, there is no possibility to connect $P_3^{(0)}$ to P_2 in this region; these solutions are classified as Class VII$_c$ in Fig. 2.

(iv) $P_3(m'_3 > -1, m > 0)$ and $P_3(m'_3 < -1, m > 0)$ to $P_8(0 < m(r = -2) < 1)$.
In this last class, there are two situations that can lead to a stable accelerated epoch. In the first one, after leaving the matter point, the trajectories go to the final attractor at the point P_8, which we refer to as Class V (Fig. 1). However, in the latter situation, before reaching the final attractor there is a "false" accelerating era in which the curve $m(r)$ meets the line $m = -r - 1$ in an unallowable region of the point P_1, in which there is no stable accelerated expansion. These solutions are labeled as Class VI (Fig. 1).

IV. CASE STUDIES

In this section, without loss of generality, we examine the discussed classification scheme by considering some well-defined specific theories for simplicity, and then investigate the possible cosmological solutions. First of all, by "well-defined" we mean the corresponding models whose $m(r)$ curves can be derived explicitly with respect to r. We do not go into the details unless there would be some new cosmological solutions with respect to $f(R)$ gravity, though to complete the discussion we may mention the other solutions wherever it is necessary. As the related models are determined by the behavior of their curves $m(r)$, our task is to find the cosmological solutions by exploring the properties of these curves. The following discussed theories are of the form $f(R,T) = g(R) + \sqrt{-T}$, where the functionality of $\sqrt{-T}$ is enforced by the conservation law, Eq. (3.6). As mentioned in Refs. [83,84], some $f(R)$ gravity models cannot pass the necessary criteria in order to have an acceptable cosmological history, e.g., a lack of a deceleration expansion period to admit a standard structure formation [85], or a quick transition from the radiation era to the late-time acceleration or the lack of a connection between the matter era and the late-time acceleration era. In this respect, the authors of

[18] We define $m'_i \equiv m'|_{P_i}$.

[19] Since the assumption $g'(R) > 0$ leads to a monotonic function $r(R)$ and hence a single valued $m(r)$, we do not consider a multivalued $m(r)$.

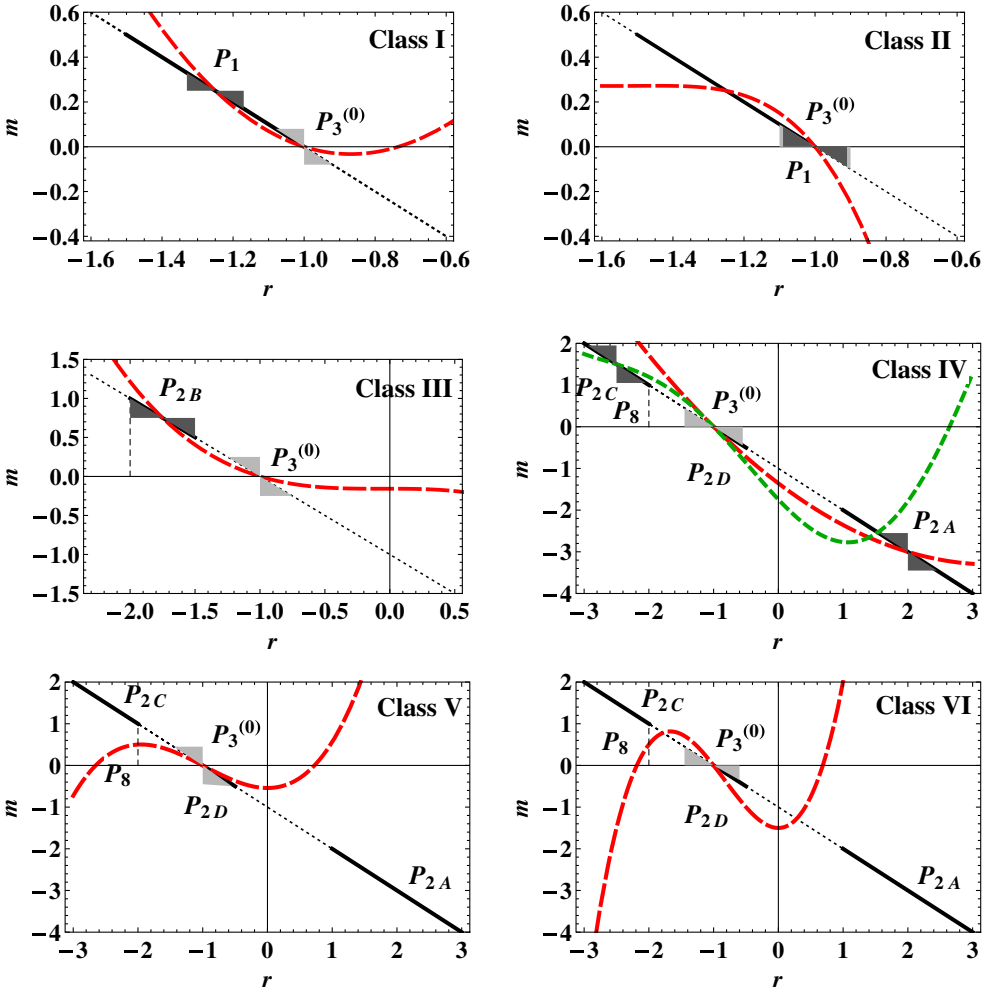

FIG. 1 (color online). Acceptable cosmological solutions of $f(R,T) = g(R) + h(T)$ gravity. The classification of the $f(R,T)$ model in the (r, m) plane. The line $m = -r - 1$ and different curves of $m(r)$ for the six classes of acceptable cosmological solutions are plotted. The transitions are depicted from the matter epoch $P_3^{(0)}$ to the accelerated point P_1 in Classes I and II, to the accelerated point P_2 in Classes III and IV, and to the de Sitter point P_8 in Classes V and VI. The matter-acceleration epoch transition occurs in Class II for the same value of r, and in Class VI before reaching to the de Sitter point P_8, with a nonstable acceleration middle stage. The solutions are permitted only in the black solid regions on the line $m = -r - 1$ provided that $m_1' < -1$, and $m_{2,\mathcal{A},\mathcal{D},\mathcal{C}}' > -1$. For P_3, we can have either $m_3' < -1$ or $m_3' > -1$ depending on the corresponding class. In Classes I, II and V we have $m_3' > -1$, whilst in the rest we have $m_3' < -1$. Unallowable slopes for the curve $m(r)$ are indicated by the light gray triangles for $P_3^{(0)}$ (actually, there is no unallowable slope for $P_3^{(0)}$; however, the light gray triangles are indicated for the sake of classification) and by the gray ones for P_1 and P_2. The dashed curves show hypothetical curves which intersect the line $m = -r - 1$ at the critical points P_1, P_3, and P_2 in the regions $\mathcal{A}$, $\mathcal{D}$, and $\mathcal{C}$. All of the classes of solutions are new ones in $f(R,T)$ gravity except for Classes III and V, which also appear in $f(R)$ gravity.

Refs. [76,83,84] have shown that theories of the form $f(R) = \alpha R^n$ and $f(R) = R^p \exp(q/R)$ do not lead to a connection between the standard matter era and the accelerated attractors. In addition to these difficulties, the authors of Ref. [76] have numerically shown that the models of type $f(R) = R^p[\log(\alpha R)]^q$ and $R^p \exp(q/R)$ suffer from a nonstandard matter era for some initial values. In the former one, the matter era is not effectively dominant, and in the latter one the standard matter era is replaced by the ϕ matter-dominated epoch (ϕMDE) epoch.[20] Hence, we reconsider the following plausible models in the background of $f(R,T)$ gravity in order to find out whether these issues can be cured. Incidentally, if m is a constant parameter, the definition (2.20) will give $g(R) \propto R^{m+1}$, i.e., a power-law function. Finally, at the end of this section, we briefly furnish the comparison of the properties of solutions for the investigated models in both $f(R,T)$ and $f(R)$ gravities in Table III.

A. $f(R,T) = aR^{-\beta} + \sqrt{-T}$, $a > 0$, $\beta \neq 0$

This theory gives $m(r) = -\beta - 1$, which intersects the line $m = -r - 1$ at $r = \beta$. As $m(r) = 0$ is valid only for

[20]The ϕMDE has been introduced in Ref. [86].

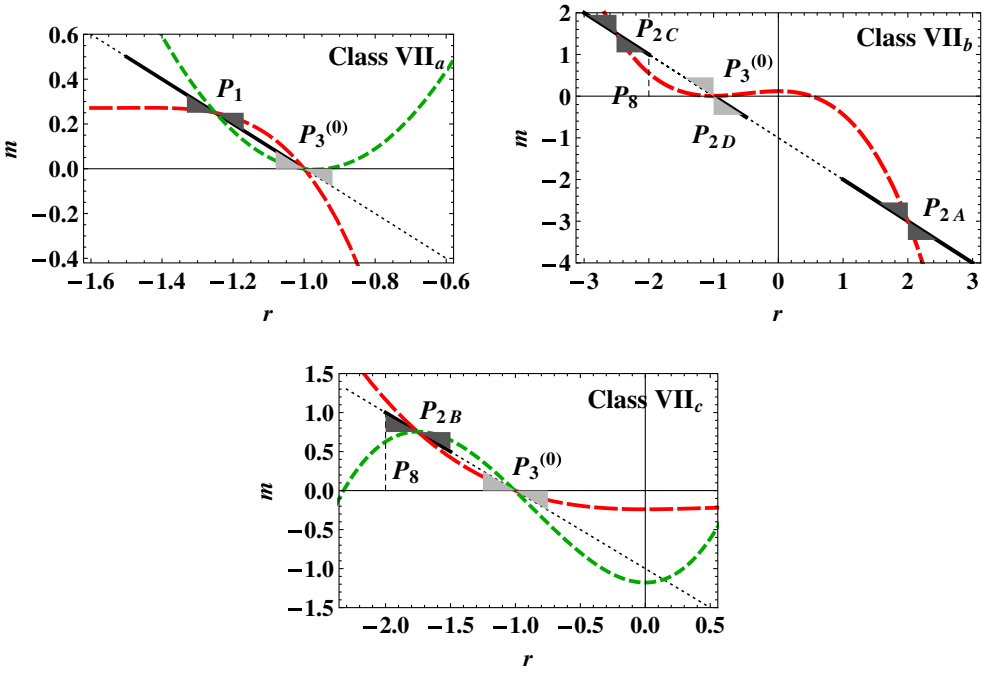

FIG. 2 (color online). Unacceptable cosmological solutions of $f(R,T) = g(R) + h(T)$ gravity. Some classes of solutions that suffer from either the absence of a matter-dominated epoch or a stable accelerated era, or unallowed transitions from the matter to the acceleration phase, are presented. There may be some other classes related to these solutions, but all of them can be classified as subclasses of those already mentioned. Again, as in Fig. 1, the dashed curves show hypothetical curves which intersect the line $m = -r - 1$.

$\beta = -1$, the condition $\mathcal{M}(r) = 0$ must be satisfied for all values of β except for $\beta = -1$. In this case, because we have $x_3 = \beta x_2$, the system reduces to a system with three degrees of freedom in which the eigenvalues of the points P_1 and P_3 are given by the first three values in Eqs. (3.19) and (3.28), respectively. To be more exact, P_1 is accelerated in $-1.50 < \beta < -1.43$ and $-1.43 < \beta < -1$, where in the first range we have a stable accelerated epoch and in the second we have a spiral stable accelerated epoch. On the other hand, for $-1.43 < \beta < -1$, this theory has a saddle matter era with a damped oscillation when $m \to 0^+$, and for the same root P_1 is a spiral stable accelerated point, which means the corresponding models belong to Class II for categorization purposes. Therefore, in the background of $f(R,T)$ gravity, this theory has a cosmological solution with a standard matter-acceleration epoch sequence, unlike $f(R)$ gravity. We illustrate three examples of this theory in Fig. 3 with the same initial values except x_3. In this case, r has a constant value with respect to time. The diagrams show some disturbances originating from the deviation of the magnitude of β from one, i.e., as $|\beta|$ deviates from one more disturbances occur. The reason is that the increase of the magnitude of β leads to the growth of the deviation of m from zero, and this in turns causes an increase in the error of matter and radiation solutions of the system of equations (3.8)–(3.11). The curves become smoother by decreasing the deviation, showing an appropriate succession of the radiation-matter-accelerated expansion eras. These examples have the point P_1 as an attractor solution with $-0.65 < w^{(\mathrm{eff})} < -0.5$. The diagrams have the present values $\Omega_0^{(\mathrm{m})} \approx 0.3$ and $\Omega_0^{(\mathrm{rad})} \approx 10^{-4}$.

B. $f(R,T) = R^p \exp(qR) + \sqrt{-T}$, $q \neq 0$

In this theory, for $r \neq 0$ we get $m(r) = -r + p/r$, $\mathcal{M}(r) = (p + r)/(p - r^2)$, and $m'(r) = -1 - p/r^2$, which are independent of q. For $r = -p$, the corresponding models do not satisfy the condition $\mathcal{M}(r) = 0$ for $p = 0$ and $p = 1$; however, for the other values of p the two conditions hold. On the other hand, for $p \approx 0$ we have $m(r) \approx -r$, and hence the condition for the existence of a matter solution $m(r \approx -1) \approx 0^+$ is not met; therefore, the pure exponential models do not have any cosmological solution. Nevertheless, in addition to $\mathcal{M}(r) \approx 0$, in order to have $m \to 0^+$ the condition[21] $r \approx -p$ for $p \to 1^+$ must hold. Actually, for this theory we have $r = -1 - qR$, and hence we get $r \to -1$ from the left-hand side only when $R \to 0^+$ with $q > 0$. Since $m_3'(p \to 1^+) < -1$ and $m_1'(-3/2 < r < -1) < -1$, it is impossible to connect $P_3^{(0)}$ to P_1 for two different roots of $m(r_i) = -r_i - 1$. One exception occurs when P_1 is the attractor solution for the same root; in such a case there is a cosmological solution which belongs to Class II. In Fig. 9, we draw a plot

[21]More precisely, $r \to -1^-$.

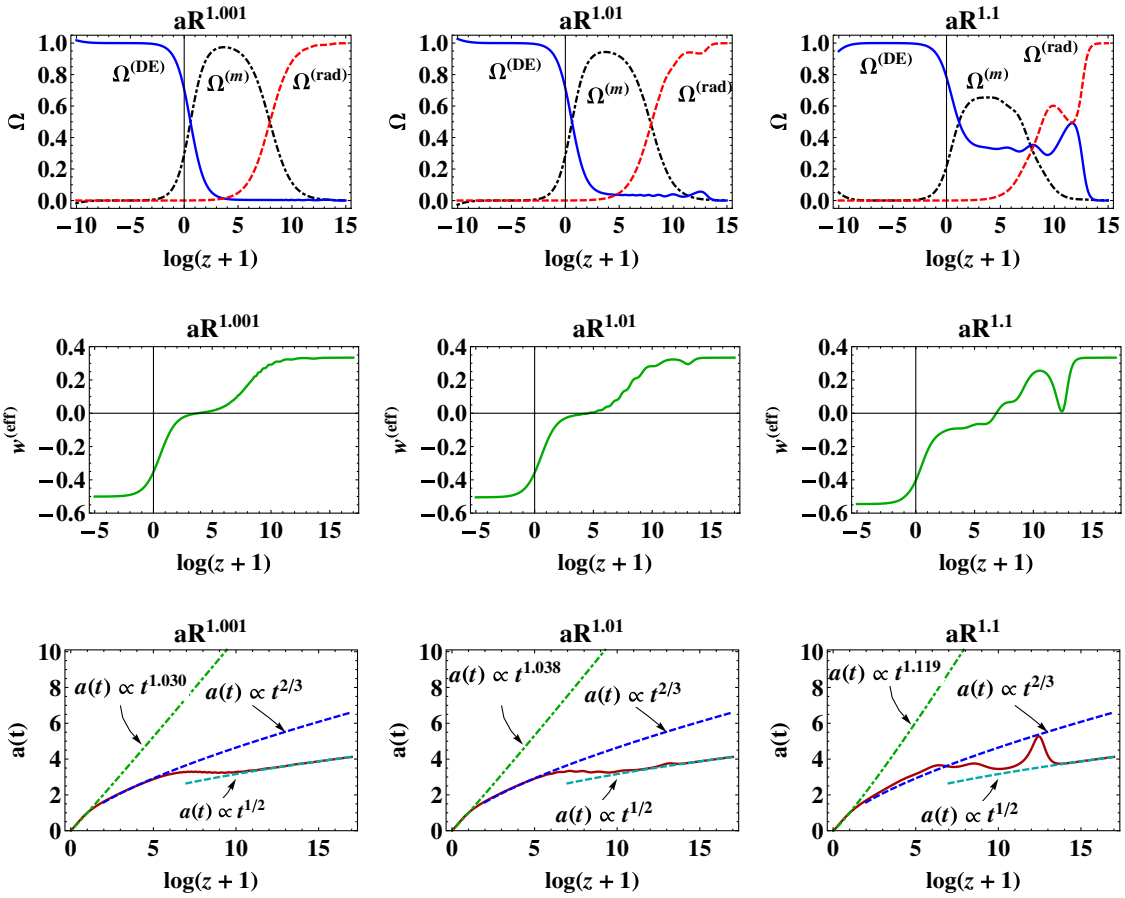

FIG. 3 (color online). Cosmological solutions of $f(R,T) = aR^{-\beta} + \sqrt{-T}$ gravity. The numerical solutions with $a > 0$ for three values of β are presented. The density parameters for various ingredients are plotted in the first row, the effective equation of state parameter in the second row, and the evolution of the scale factor in the last row. The diagrams are plotted for the initial values $x_1 = 10^{-4}, x_2 = -10^{-4}, x_3 = -\beta \times 10^{-4}, x_4 = 10^{-13}$, and $x_5 = 0.999$, corresponding to $z \approx 2.42 \times 10^7$. The diagrams are made to be consistent with $\Omega_0^{(m)} \approx 0.3$ and $\Omega_0^{(rad)} \approx 10^{-4}$ at the present epoch; however, they give $-0.65 < w^{(eff)} < -0.5$ instead of $w^{(eff)} \to -1$. The peak of $\Omega^{(m)}$ decreases with a change in β, i.e., as β increases the diagrams get tangled up. Such disorderings are indicated in the diagrams of $w^{(eff)}$ and in the deviations of the behavior of the scale factor in the matter epoch from its standard form $a \propto t^{2/3}$. The best solutions are achieved for $\beta \to -1$.

for the $m(r)$ curve for this theory in the plane (r, m) with $p = 1.001$. Also, to illustrate the idea, we numerically depict interesting cosmological quantities predicted by this theory in Fig. 4 for $p = 1.001$ and the initial value $r_i = -1.002$ in order to have the present values $\Omega_0^{(m)} \approx 0.3$ and $\Omega_0^{(rad)} \approx 10^{-4}$.

C. $f(R,T) = R + \alpha R^{-n} + \sqrt{-T}, n \neq 0$

For this theory, we obtain $m(r) = -n(1+r)/r$ and $\mathcal{M}(r) = 1 - r/n$,[22] which show that the condition $\mathcal{M}(r) = 0$ is satisfied only for $r = n$, which in turn gives $m \neq 0$. On the other hand, the corresponding models contain the matter point $P_3^{(0)}$ when $r = -1$, which means that only models with $n = -1$ can be accepted. However, we describe the properties of solutions for values of n approaching -1 in the following models [where in these cases we have $\mathcal{M}(r = -1) \approx 0$].

(i) Models with $n \to -1^-$.
In these cases, the equation $m(r_i) = -r_i - 1$ has two roots, i.e., $r_{1,2} = -1, n$. Generally, we have $m'(r) = n/r^2$, and as a result, for the initial values $r_i < \sqrt{|n|}$, we have $m_3' < -1$ and $m_1' > -1$, which make P_1 a saddle point. Thus, since $m(r = -2) = -n/2$, these solutions accept the de Sitter point P_8 as the final attractor after a transition from the saddle point P_1. These models belong to Class VI. On the other hand, for $-\sqrt{|n|} < r_i < -1$, the point P_1 is a stable point. These solutions belong to Class II. In Fig. 5, we plot the related diagrams of the $R + \alpha R^{1.1}$

[22] In obtaining the equation $\mathcal{M}(r) = 1 - r/n$, we assume $r \neq -1$; however, after removing the ambiguity at $r = -1$, it gives $\mathcal{M}(r = -1) = 1 + 1/n$.

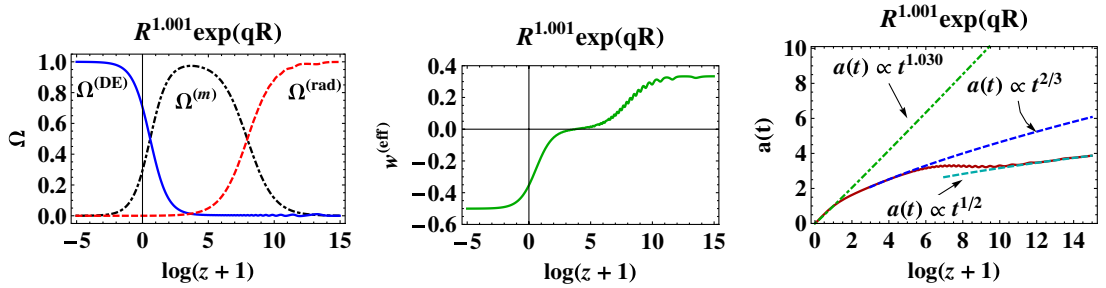

FIG. 4 (color online). Cosmological solutions of $f(R,T) = R^p \exp(qR) + \sqrt{-T}$ gravity. The plots are presented for $p = 1.001$ and the initial values $x_1 = 10^{-4}$, $x_2 = -10^{-4}$, $x_3 = 1.002 \times 10^{-4}$, $x_4 = 3.8 \times 10^{-13}$, and $x_5 = 0.999$, corresponding to $z \approx 3.17 \times 10^6$. The diagram of $w^{(\mathrm{eff})}$ shows that the final attractor solution is P_1. The present values of the density parameters are extrapolated as $\Omega_0^{(\mathrm{m})} \approx 0.3$ and $\Omega_0^{(\mathrm{rad})} \approx 10^{-4}$.

model. In this example, the initial value $r_i = -1.0008$ is applied in such a way that it chooses P_1 as the final attractor and also gives the present values for the Ω's. In Fig. 9, we also present the $m(r)$ curve for this example.

(ii) Models with $n \longrightarrow -1^+$.
For models with $n \longrightarrow -1^+$, the initial conditions $r_i > -\sqrt{|n|}$ are not allowed, for these conditions lead to $m \approx 0^-$, which is physically ruled out. However, the initial values $r_i < -1$ are allowed

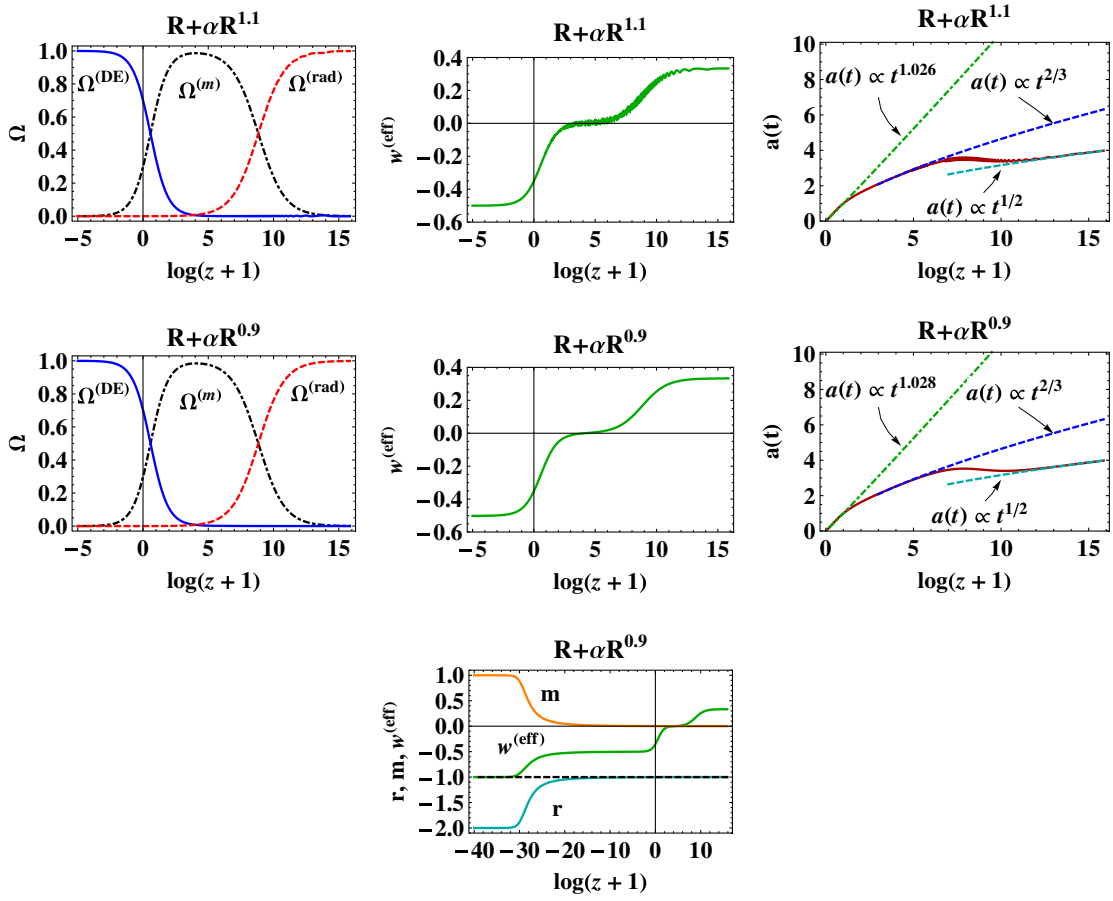

FIG. 5 (color online). Cosmological solutions of $f(R,T) = R + \alpha R^{-n} + \sqrt{-T}$ gravity. The diagrams are for $n = -1.1$ and the initial values $x_1 = 10^{-4}$, $x_2 = -10^{-5}$, $x_3 = 1.0008 \times 10^{-5}$, $x_4 = 10^{-13}$, and $x_5 = 0.999$, corresponding to $z \approx 7.65 \times 10^6$. The model matches with the present observational data $\Omega_0^{(\mathrm{m})} \approx 0.3$ and $\Omega_0^{(\mathrm{rad})} \approx 10^{-4}$; however, its $w^{(\mathrm{eff})}$ converges to -0.5 instead of -1. There is a desirable succession of radiation-matter-acceleration phases. The scale-factor evolution curve has the asymptotic form of $a \propto t^{1/2}$ at high redshifts and behaves as $a \propto t^{2/3}$ when the matter becomes dominant. The model with $n = -0.9$ is plotted for the same initial values except for $x_2 = -10^{-4}$ and $x_3 = 1.00002 \times 10^{-4}$. This model shows a transition from a temporal acceleration epoch to the final attractor in the vicinity of P_8, and hence it belongs to Class VI.

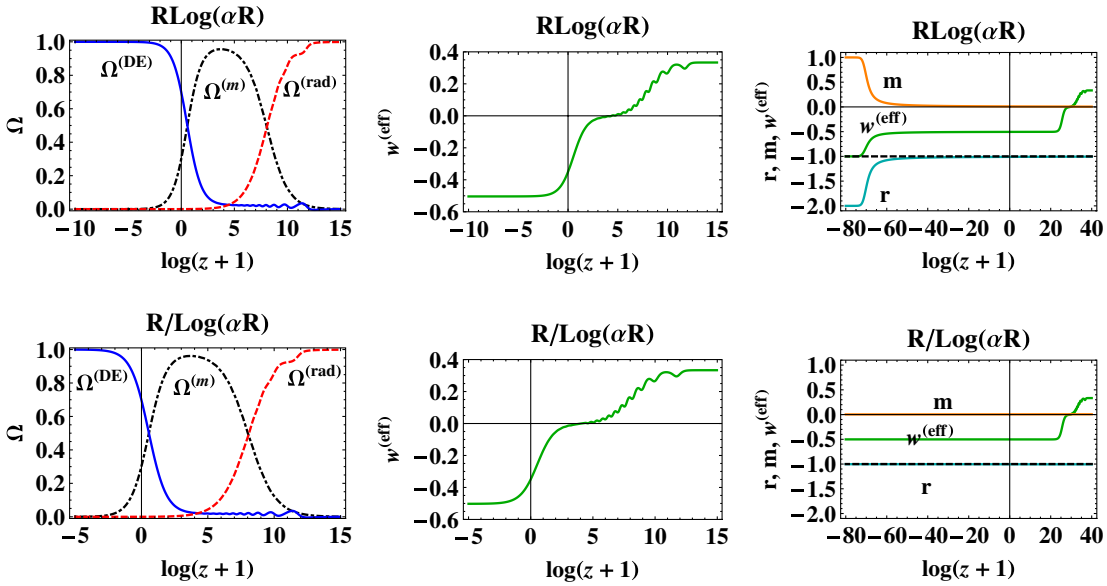

FIG. 6 (color online). Cosmological solutions of $f(R,T) = R(\log \alpha R)^q + \sqrt{-T}$ gravity. The diagrams for the density parameter and the effective equation of state parameter are plotted for two values, $q = 1$ and $q = -1$. The diagrams for m, r, and $w^{(\mathrm{eff})}$ are drawn in a wide range of redshift. The Ω's show admissible behaviors in both cases. In the right panel, the first-row diagrams shows a transition from a saddle accelerated epoch with $w^{(\mathrm{eff})} \approx -0.5$ to a stable one with $w^{(\mathrm{eff})} \approx -1$ for $q = 1$. All three diagrams support this result. Unlike $R \log \alpha R$, the theory $R/\log \alpha R$ does not show these transitions. We draw the $m(r)$ curve for the model $R \log \alpha R$ in Fig. 9, which indicates that this theory belongs to Class VI. The $m(r)$ curves of the theory first intersect the line $m = -r - 1$ in an unallowed region, then the line $r = -2$ as a final attractor. The diagrams are plotted for the initial values $x_1 = 10^{-10}$, $x_2 = -10^{-7}$, $x_3 = 1.0058 \times 10^{-7}$, $x_4 = 4 \times 10^{-13}$, and $x_5 = 0.999$, corresponding to $z \approx 3.17 \times 10^6$ for both theories. The diagrams represent the values of $\Omega_0^{(\mathrm{m})} \approx 0.3$ and $\Omega_0^{(\mathrm{rad})} \approx 10^{-4}$ at the present epoch.

and give $m_1' > -1$. Therefore, in these models the universe, after passing a matter-dominated, is trapped in a temporal accelerated expansion state that is determined by P_1 and then chooses P_8 as a final de Sitter attractor. These models belong to Class VI. In the numerical considerations we have chosen $r_i = -1.00002$, which results in an acceleration in a transient period by P_1, then a permanent accelerated expansion by P_8 (see Fig. 5).

In the cases with $n \to -1^-$, cosmological solutions exist only for $\alpha > 0$ in the limit $R \to 0$, whilst the cases with $n \to -1^+$ have solutions provided that $\alpha < 0$ and $R \to \infty$ because $m = n(n+1)\alpha R^{-n-1}/(1 - n\alpha R^{-n-1})$. In $f(R)$ gravity these models can have cosmological solutions only when $-1 < n < 0$; however, in $f(R,T)$ gravity, in addition to these solutions, there are acceptable solutions for $n \to -1^-$ as well.

D. $f(R,T) = R^p[\log(\alpha R)]^q + \sqrt{-T}$, $q \neq 0$, $\alpha > 0$

This theory has the following functions:

$$m(r) = \frac{(p+r)^2 - qr(1+r)}{qr} \quad \text{and} \quad \mathcal{M}(r) = \frac{(p+r)^2}{(p+r)^2 - qr(1+r)}, \tag{4.1}$$

where $r \neq 0$. The condition $\mathcal{M}(r) = 0$ holds for $r = -p$; however, only for $p = 1$ do we have $m(r) = 0$ for $r = -1$.[23] Incidentally, for $p = 1$ and $m(r = -2) = 1 - 1/2q$ the point P_8 is a stable accelerated attractor for $q > 1/2$. Generally, in this theory there are three situations in which the matter solution $m \to 0^+$ can be obtained, namely,

i) $q > \dfrac{1+r}{r}$, $r \to -1^- \Rightarrow m' > -1$,

ii) $q < 0$, $r \to -1^- \Rightarrow m' < -1$,

iii) $\dfrac{1+r}{r} < q < 0$, $r \to -1^+ \Rightarrow m' > -1$.

The first situation shows that the corresponding models for $0 < q < 1/2$ with $m_{1,3}' > -1$ lie in Class VII$_a$. On the other hand, P_2 cannot be the final attractor because the curve $m(r)$ does not have any root in the regions $\mathcal{A}$, $\mathcal{B}$, $\mathcal{C}$, and $\mathcal{D}$. However, for $q > 1/2$ the final attractor is P_8. The corresponding models in the second situation, in which $m_{1,3}' < -1$, lie in Class II for the same root r, as represented in Fig. 5, but the transition to $P_{2\mathcal{B}}$ does not lead to a good cosmological solution, which lies in Class VII$_c$. In the last situation, the range of q gets narrowed as r approaches -1, and hence it is of less importance for our studies.

[23]Note that the existence of the matter point for all types of this case is independent of q.

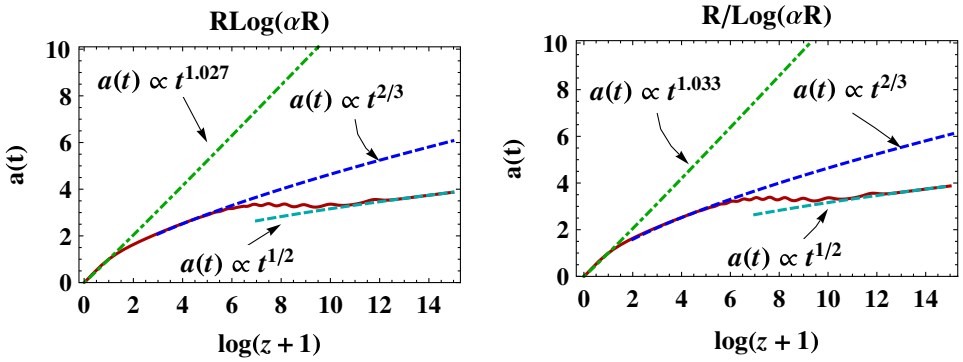

FIG. 7 (color online). The scale-factor evolution curves for the two theories with $g(R) = R\log\alpha R$ and $g(R) = R/\log\alpha R$ are depicted. The asymptotic lines show the behaviors of the scale factor at the high-redshift regime, in the matter-dominated epoch and at late times.

In Figs. 6 and 7, we plot two examples of such cases for $q = \pm 1$. Both examples show an acceptable succession of the radiation-matter-accelerated expansion eras. The theory $R\log\alpha R$ belongs to Class VI, which has P_8 as the final attractor. In addition to the curves of the density parameters for the radiation, matter, and acceleration eras, the curves of $r \equiv -Rg'/g$, $m \equiv Rg''/g'$ and the effective equation of state are depicted. These curves show a transition from the saddle accelerated point P_1 to a stable de Sitter acceleration expansion phase after a long time. Figure 6 shows that the curve $m(r)$ first intersects the line $m = -r - 1$ in regions $r \longrightarrow -1^-$, in which P_1 is a saddle point, and then intersects the line $r = -2$ where P_8 is a stable point. Therefore, these solutions belong to Class VI. Also, $w^{(\mathrm{eff})}$ makes a transition from a nonphantom accelerating era with the value $w^{(\mathrm{eff})} \approx -1/2$ to a de Sitter epoch with $w^{(\mathrm{eff})} \approx -1$. Unlike this theory, the other theory, i.e., $R/\log(\alpha R)$, has P_1 as the only attractor, as seen from Fig. 6. The latter theory belongs to Class II.

We conclude that the corresponding models of $g(R) = R^p[\log(\alpha R)]^q$ are cosmologically acceptable for $p = 1$ with $q < 0$ and $q > 1/2$ in the background of $f(R,T)$ gravity, whereas in $f(R)$ gravity the solutions exist only in the range $q > 0$.

E. $f(R,T) = R^p \exp(q/R) + \sqrt{-T}$

This theory has the relations

$$m(r) = -\frac{p + r(2 + r)}{r} \quad \text{and} \quad \mathcal{M}(r) = \frac{p + r}{p + r(2 + r)}, \tag{4.2}$$

where $r \neq 0$. The condition $\mathcal{M}(r) = 0$ is satisfied when $r = -p$ and for all values of p except $p = 0$, 1. On the

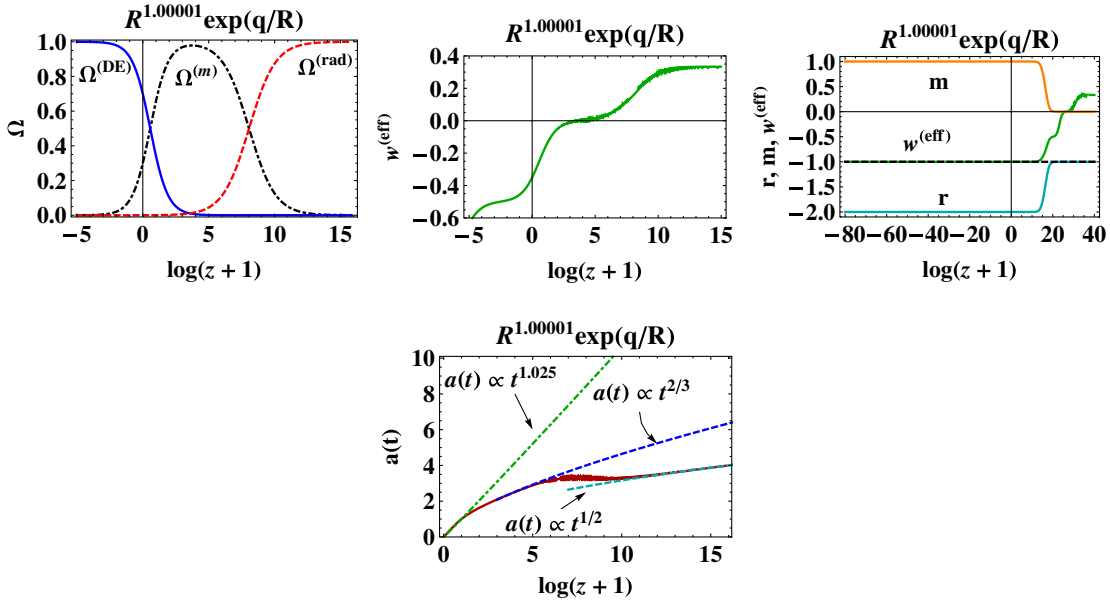

FIG. 8 (color online). Cosmological solutions of $f(R,T) = R^p \exp(q/R) + \sqrt{-T}$ gravity. The plots are provided for $p = 1.00001$ and the initial values $x_1 = 10^{-5}$, $x_2 = -10^{-25}$, $x_3 = 1.00001 \times 10^{-25}$, $x_4 = 10^{-15}$, and $x_5 = 0.9999$, corresponding to $z \approx 3.53 \times 10^7$. In this case, one always has $m_1' > -1$, which means that P_8 is the final attractor.

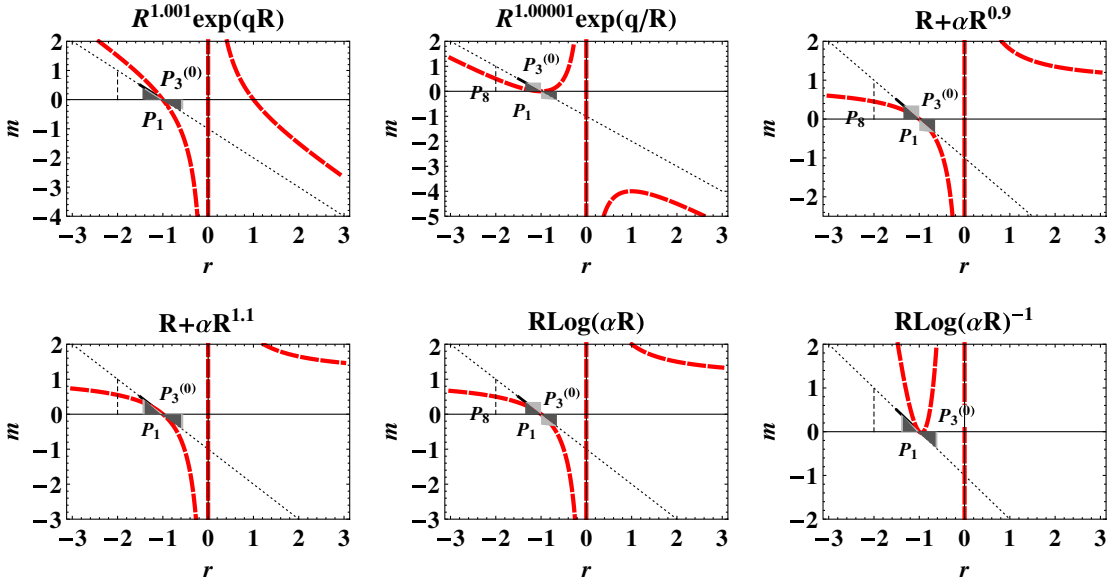

FIG. 9 (color online). Theoretical curves for $m(r)$ for some models in $f(R,T)$ gravity. The $m(r)$ curves are illustrated for some models corresponding to the represented classifications. Contrary to $f(R)$ gravity, the existence of the new point P_1 and the new stability condition for P_3 ($P_3^{(0)}$ is a saddle point for both $m' < -1$ and $m' > -1$) bring about the appearance of new acceptable solutions. The models for which P_8 is the final attractor (indicated by the two opposite triangles sets) belong to Class V, and those for which P_1 is the final attractor (indicated by the two fitted triangles sets) belong to Class I.

other hand, the matter era only exists in $r = -p = -1$, and hence we consider the theory in $r = -p$ when $p \to 1^+$. In this situation we have $m_1' > -1$, and therefore the point P_1 cannot be stable, while P_2 can be a stable accelerated point in the region $\mathcal{C}$. Since $m''(r) = -2p/r^3$ the point $(r \approx -1,\ m \approx 0)$ is a minimum with a positive concavity. Note that for $r < -1$ we have $m(r) < -r - 1$, which has an asymptotic behavior in $r \to -\infty$ as $m(r) \to -r$. Since $r = (q/R) - 1$ in this theory, the latter behavior occurs for $q < 0$ and $R \to 0^+$, which means that $P_{2\mathcal{C}}$ can be the final attractor. However, the trajectories have already been trapped by P_8 in a finite r. In this theory—like the corresponding models of $R\log(\alpha R)$—before reaching the final attractor in P_8 there is a short time interval in which the trajectories pass by P_1 (which is a saddle point). Thus its corresponding models belong to Class VI.

As a result, the corresponding models, in general, have cosmological solutions provided that $q < 0$ for $R \to \infty$. In Fig. 8, we depict a numerical calculated example for these models provided we have the present observed values for the density parameters. This example belongs to Class VI, as is obvious by comparing it with the solutions of Class VI (Fig. 1) with the corresponding curve $m(r)$ in Fig. 9.

V. PURE NONMINIMAL CASE $f(R,T) = g(R)h(T)$

Since we propose to investigate a pure nonminimal case in this section, one should be more careful about the functionality of $h(T)$. Indeed, in the vacuum state we do not want to have a null Lagrangian. Stated loosely, there should be a solution for the vacuum state (contrary to the strong version of the Mach idea). Therefore, in this nonminimal case the following assumption is necessary:

$$\lim_{T\to 0} h(T) \neq 0. \tag{5.1}$$

Furthermore, for simplicity in this and the following sections, we only consider dust-like matter. Using the definitions presented in Sec. II [Eqs. (2.12) and (2.13)], we get

$$1 + \frac{1}{6}\frac{g}{H^2 g'} - \frac{1}{6}\frac{R}{H^2} + \frac{\dot{g}'}{Hg'} + \frac{\dot{h}}{Hh} = \frac{8\pi G\rho^{(\mathrm{m})}}{3H^2 g' h} + \frac{gh'\rho^{(\mathrm{m})}}{3H^2 g' h} \tag{5.2}$$

and

$$2\frac{\dot{H}}{H^2} + \frac{\ddot{g}'}{H^2 g'} + 2\frac{\dot{g}'}{Hg'}\frac{\dot{h}}{Hh} + \frac{\ddot{h}}{H^2 h} - \frac{\dot{g}'}{Hg'} - \frac{\dot{h}}{Hh} = -\frac{8\pi G\rho^{(\mathrm{m})}}{H^2 g' h} - \frac{gh'\rho^{(\mathrm{m})}}{H^2 g' h}. \tag{5.3}$$

Rewriting the first equation with respect to the defined variables and parameters (2.14)–(2.16) and (2.23) gives

$$\Omega_{\mathrm{p.n.}}^{(\mathrm{m})} = 1 - x_1 - x_2 - x_3 - s(3 + 2x_2), \tag{5.4}$$

where we have defined the corresponding pure nonminimal matter-density parameter as

$$\Omega_{\mathrm{p.n.}}^{(\mathrm{m})} \equiv \frac{8\pi G\rho^{(\mathrm{m})}}{3H^2 g' h}. \tag{5.5}$$

In the above definition for $\Omega_{\mathrm{p.n.}}^{(\mathrm{m})}$, the existence of the function $h(T)$ warns us about the sign of $\Omega_{\mathrm{p.n.}}^{(\mathrm{m})}$. That is,

TABLE III. Cosmological solutions of $f(R,T)$ gravity compared with $f(R)$ gravity.

Theory	$f(R,T)$ gravity				$f(R)$ gravity	
$g(R)$ Model	Class II	Class VI	Class VII$_a$	Class VII$_b$	Class V	Class VII$_b$
$aR^{-\beta}$, $a>0$	$-1.43<\beta<-1$					$-0.713<\beta<-1$
$R^p \exp qR$	$p\to 1^+$, $q>0$			$p\approx 0$		$p=0$, $p=1$
$R+\alpha R^{-n}$	n[a]$\to -1^-$	$n\to -1^+$, $n\to -1^-$			$-1<n<0$, $\alpha<0$	
$R^p(\log \alpha R)^q$	$p=1$, $q<0$	$p=1$, $q>1/2$	$p=1$, $0<q<1/2$		$p=1$, $q>0$	$p\neq 1$
$R^p \exp q/R$		$p\to 1^+$, $q<0$			$p=1$	$p\neq 1$

[a]For models with $n\to -1^-$, we have $\alpha>0$ and for models with $n\to -1^+$, we have $\alpha<0$.

as we have only assumed that $g'(R)>0$, the density parameter $\Omega^{(\mathrm{m})}_{\mathrm{p.n.}}$ may obtain negative values due to the appearance and functionality of $h(T)$. On the other hand, if one physically demands that $\Omega^{(\mathrm{m})}_{\mathrm{p.n.}}$ must be positive, then the functionality of $h(T)$ will be restrictive, e.g., an exponential function.

We have three dynamical equations for x_1, x_2, and x_3; the equations for x_2 and x_3 are the same as Eqs. (3.9) and (3.10), respectively. However, the equation for x_1 changes as

$$\frac{dx_1}{dN} = -1 + x_1(x_1 - x_3) - 3x_2 - x_3 + 3s(2x_1 - x_3 + 3s). \tag{5.6}$$

In addition to the EOM constructed by Eqs. (3.9), (3.10), and (5.6) we have a constraint due to the energy-momentum conservation law. It is easy to check that the constraint (2.11) leads to the following relations between the parameters n and s with the other variables:

$$n = \frac{x_1 x_3}{3m x_2} - \frac{1}{2} \tag{5.7}$$

and

$$s = \frac{x_1 x_3}{3m x_2} + \frac{1}{2}, \tag{5.8}$$

which in turn specify the functionality of $h(T)$ and create a complicated relation between $g(R)$ and $h(T)$. Indeed, further investigations indicate that $h(T)$ is a complicated exponential function of T, which guaranties that $\Omega^{(\mathrm{m})}_{\mathrm{p.n.}}$ is positive. However, we have a dynamical system with three variables and two constraints, this system of equations accepts four fixed points, which are summarized in Table IV.

The most important point that can be observed is that the matter-density parameters of all the fixed points are zero. There is no solution to describe a standard matter-dominated era. Thus, we do not consider the general properties of their fixed points and (henceforth) their stabilities. However, the properties of each point can be briefly summarized. The point P_1 is a nonstandard matter era, as the condition $w^{(\mathrm{eff})}=0$ is satisfied in $m=-2$ but we have $\Omega^{(m)}_{\mathrm{p.n.}}=0$. P_1 is a de Sitter point when $m=0.6$. For this point, the nonphantom accelerating expansion occurs when $0.48<m<0.60$, and the phantom accelerating expansion occurs when $m>0.6$. The point P_2 can expand the universe in the range $0.48<m<1.40$ in the nonphantom domain and in the range $m<-1$ in the phantom domain. The point P_3 is a special case of the point P_1 when $m=0.6$, which is a de Sitter point. And—contrary to our initial assumption for the investigation of this theory—the point P_4 resembles a radiation point, which is not physically justified.

VI. NONMINIMAL CASE $f(R,T) = g(R)(1 + h(T))$

Since a general Lagrangian $L = g_1(R) + g_2(R)h(T)$ makes the calculations and the stability considerations more complicated, we will just study the nonminimal case $f(R,T) = g(R)(1 + h(T))$.

The following field equations are obtained:

$$1 + \frac{1}{6}\frac{g}{H^2 g'} - \frac{1}{6}\frac{R}{H^2} + \frac{\dot{g}'}{H g'} + \frac{2\dot{h}}{H(1+2h)} = \frac{8\pi G\rho^{(\mathrm{m})}}{3H^2 g'(1+2h)} + \frac{2gh'\rho^{(\mathrm{m})}}{3H^2 g'(1+2h)} \tag{6.1}$$

and

TABLE IV. The fixed-point solutions of $f(R,T) = g(R)h(T)$ gravity without radiation.

Fixed point	Coordinates (x_1, x_2, x_3)	Parameter s	$\Omega^{(m)}_{\mathrm{p.n.}}$	$w^{(\mathrm{eff})}$
P_1	$\left(\frac{m(5-m-a_m}{4(1+m)}, -\frac{11+17m+a_m}{8(1+m)^2}, \frac{11+17m+a_m}{8(1+m)}\right)$[a]	$\frac{1}{12}(1+m+a_m)$	0	$-\frac{7+13m+a_m}{12(1+m)}$
P_2	$\left(\frac{m(5-m+a_m)}{4(1+m)}, -\frac{11+17m-a_m}{8(1+m)^2}, \frac{11+17m-a_m}{8(1+m)}\right)$	$\frac{1}{12}(1+m-a_m)$	0	$-\frac{7+13m-a_m}{12(1+m)}$
P_3	$(0, -\frac{5}{4}, 2)$	0	0	-1
P_4	$(-4, -\frac{7}{4}, 0)$	0	0	$\frac{1}{3}$

[a]Where $a_m \equiv \sqrt{-47+38m+121m^2}$.

$$2\frac{\dot{H}}{H^2}+\frac{\ddot{g}'}{H^2g'}+\frac{\dot{g}'}{Hg'}\frac{4\dot{h}}{H(1+2h)}+\frac{2\ddot{h}}{H^2(1+2h)}-\frac{\dot{g}'}{Hg'}-\frac{2\dot{h}}{H(1+2h)}=-\frac{8\pi G\rho^{(\mathrm{m})}}{H^2g'(1+2h)}-\frac{2gh'\rho^{(\mathrm{m})}}{H^2g'(1+2h)}. \tag{6.2}$$

To get the dynamical equation from Eqs. (6.1) and (6.2), we need to define a new variable,

$$y\equiv\frac{h}{1+2h}. \tag{6.3}$$

Hence, the corresponding nonminimal matter-density parameter satisfies

$$\Omega_{n.}^{(\mathrm{m})}=1-x_1-x_2-x_3-2s(3+2x_2)y, \tag{6.4}$$

where

$$\Omega_{n.}^{(\mathrm{m})}\equiv\frac{8\pi G\rho^{(\mathrm{m})}}{3H^2g'(1+h)}. \tag{6.5}$$

Owing to these variables, the dynamical equations for x_1 and x_4 are derived as

$$\frac{dx_1}{dN}=-1+x_1(x_1-x_3)-3x_2-x_3+6s(2x_1-x_3+3s)x_4, \tag{6.6}$$

$$\frac{dx_4}{dN}=-3sx_4(1-2x_4), \tag{6.7}$$

where the corresponding equations for x_2 and x_3 remain unchanged, i.e., Eqs. (3.9) and (3.10). In addition, the parameters n and s are also the same as in Eqs. (5.7) and (5.8), which constrain the variables x_1, x_2, and x_3. The fixed points of this system are represented in Table V.

In this theory, the point P_1 contains a matter-dominated era, and the other points give de Sitter points and the accelerating expansion domains. Nevertheless, it remains to be shown that the matter point is a saddle point and that we have a stable accelerating point for the late-time acceleration of universe. In what follows, we only consider the properties of each fixed point in turn to check these possibilities. More studies on the possible cosmological solutions for some specific models can be carried out; however, this is beyond the scope of this work.

(i) P_1

This point has the following eigenvalues:

$$-\frac{1}{2},\quad\frac{-3m+\sqrt{m(256m^3+160m^2-31m-16)}}{4m(1+m)},\quad\frac{-3m-\sqrt{m(256m^3+160m^2-31m-16)}}{4m(1+m)},\quad 3(1+m'). \tag{6.8}$$

The point P_1 is a stable point when $m'<-1$ and $0<m<0.346$, and otherwise it is a saddle point. If $m'=0$, it will be a saddle point for all values of m. Also, when $m\to 0^+$ it is a saddle point provided that $m'>-1$. This point has a similar property as the corresponding one in $f(R)$ gravity.

(ii) P_2, P_5, and P_6

These three points can only play the role of attractor solutions of the system, for we have $\Omega_{P_{2,5,6}}^{(\mathrm{m})}=0$. The eigenvalues of P_2 are given as

$$-4+\frac{1}{m},\quad\frac{-8m^2-3m+2}{m(1+2m)},\quad\frac{2(1-m^2)(1+m')}{m(1+2m)},\quad\frac{10m^2+3m-4}{6m(1+2m)}. \tag{6.9}$$

When $m<(-1-\sqrt{3})/2$ or $(-1+\sqrt{3})/2<m<1$ the point P_2 can accelerate the expansion of universe in the nonphantom domain, and when $-1/2<m<0$ or $m>1$ in the phantom domain. There is no stable solution for the phantom accelerating expansion; however, the stable nonphantom accelerating domains are determined by

$$m'<-1,\qquad 0.347\lesssim m<1/2,\qquad -1/3<w^{(\mathrm{eff})}<-0.260. \tag{6.10}$$

TABLE V. The fixed points of the theory $f(R,T)=g(R)(1+h(T))$ without radiation.

Fixed point	Coordinates (x_1, x_2, x_3, x_4)	$\Omega_{n.}^{(m)}$	$w^{(\mathrm{eff})}$
P_1	$\left(\frac{3m}{1+m}, -\frac{1+4m}{2(1+m)^2}, \frac{1+4m}{2(1+m)}, 0\right)$	$\frac{2-m(3+8m)}{2(1+m)^2}$	$-\frac{m}{1+m}$
P_2	$\left(\frac{2(1-m)}{1+2m}, \frac{1-4m}{m(1+2m)}, -\frac{(1-4m)(1+m)}{m(1+2m)}, 0\right)$	0	$\frac{2-5m-6m^2}{3m(1+2m)}$
P_3	$(-4, 5, 0, 0)$	0	$\frac{1}{3}$
P_4	$(0, -1, 2, 0)$	0	-1
P_5	$\left(\frac{m(5-m-a_m)}{4(1+m)}, -\frac{11+17m+a_m}{8(1+m)^2}, \frac{11+17m+a_m}{8(1+m)}, \frac{1}{2}\right)$	0	$-\frac{7+13m+a_m}{12(1+m)}$
P_6	$\left(\frac{m(5-m+a_m)}{4(1+m)}, -\frac{11+17m-a_m}{8(1+m)^2}, \frac{11+17m-a_m}{8(1+m)}, \frac{1}{2}\right)$	0	$-\frac{7+13m-a_m}{12(1+m)}$
P_7	$(0, -\frac{5}{4}, 2, \frac{1}{2})$	0	-1
P_8	$(-4, \frac{7}{4}, 0, \frac{1}{2})$	0	$\frac{1}{3}$

In the limit $m \to 0$, the eigenvalues approximately read as

$$\frac{1}{m}, \qquad \frac{2}{m}, \qquad \frac{2}{m}(1+m'), \qquad -\frac{2}{3m}, \quad (6.11)$$

which means that for both $m \to 0^+$ and $m \to 0^-$ this point is a saddle point. Also, in the models with $m' = 0$ the point P_2 is a saddle point for all values of m.

The point P_5 can accelerate the expansion of the universe in the nonphantom domain with $-1 < w^{(\mathrm{eff})} \lesssim -0.75$ for $0.486 \lesssim m < 0.6$, and in the phantom domain with $w^{(\mathrm{eff})} < -1$ for $m > 0.6$. P_5 is stable in the first range provided that $m' < -1$, and in the second range when $m' > -1$. Finally, P_6 is always a saddle point in the nonphantom range $0.486 \lesssim m < 1.4$ and in the phantom range $m < -1$ for all values of m'.

(iii) P_4 and P_7

The eigenvalues of P_4 are given by

$$-3, \qquad \frac{1}{2}, \qquad \frac{1}{2}\left(-3-\sqrt{25-\frac{16}{m}}\right), \qquad \frac{1}{2}\left(-3+\sqrt{25-\frac{16}{m}}\right). \quad (6.12)$$

Clearly, P_4 is a saddle de Sitter point. However, the numerical calculations show that the point P_7 is a stable de Sitter solution for $0 < m < 1/2$.

We conclude this section with the assertion that the nonminimal coupling Lagrangian $f(R,T) = g(R) \times (1 + h(T))$ can have cosmological solutions in the form of transitions of P_1 to any of the points P_2, P_5, or P_7. Note that the fixed points P_3 and P_8 have $w^{(\mathrm{eff})} = 1/3$ which means that they are not physically justified in the absence of radiation.

VII. CONCLUDING REMARKS

In this work we considered the cosmological solutions of the $f(R,T)$ theory of gravity for a perfect fluid in a spatially flat, homogeneous, and isotropic background FLRW metric via the (r,m)-plane analysis. We included the dust matter and radiation in the action. We investigated some families of this theory that can be written as a combination of a pure function of the trace, e.g., $h(T)$, and a pure function of the Ricci scalar, e.g., $g(R)$, by virtue of which one is able to use $f(R,T)$ gravity as a modification of the $f(R)$ dark energy models. In Ref. [76], by introducing two dimensionless parameters r and m, the (r,m)-plane method has been employed to parametrize the $f(R)$ function and simplify the calculations. In this work, we extended their idea to the function $h(T)$ and introduced another two new dimensionless parameters, namely, n and s. With these definitions, we considered the cosmological solutions of three general theories with the Lagrangians of minimal, pure nonminimal, and nonminimal couplings via the dynamical systems approach. The conservation of the energy-momentum tensor leads to a constraint equation that relates n to the other dynamical variables, and all acceptable cosmological solutions must respect it.

In minimal gravity, this constraint confines the function $h(T)$ to a particular form, i.e., $h(T) = \sqrt{-T} + \text{constant}$. This theory gets specific values for the two new parameters, i.e., $n = -1/2 = -s$, and contains six classes of acceptable cosmological solutions and three unacceptable ones with the following remarks, particularly in comparison with the $f(R)$ gravity studied in Ref. [76].

(i) In all of the solutions, the comparison of the value of the slope of the $m(r)$ curve to -1 is of great importance. This comparison determines the acceptability of the solutions from the cosmological point of view, i.e., there should exist a succession of a saddle radiation era, a saddle matter era, and finally a stable accelerated expansion era.

(ii) For all of the fixed points, one of the three conditions (3.18) must be satisfied.

(iii) There is a matter era solution, i.e., P_3, that is always a saddle point, which exists for $m \to 0^+$ with both $m'(r) < -1$ and $m'(r) > -1$. In $f(R)$ gravity this fixed point is not allowed for $m'(r) < -1$.

(iv) There is an important fixed point, i.e., P_1, with the property $\Omega^{(m)} = 0$ which acts as a stable accelerated expansion point, in addition to the one that already exists in $f(R)$ gravity. This fixed point is the final attractor in most models of the minimal coupling theory. However, the relevant conditions for this point are

$$m'(r) < -1 \quad \text{and} \quad 0 < m < 1/2.$$

(v) There is a saddle point that indicates a "false" matter era whose scale factor does not behave like the one of the matter era (actually, its scale factor behaves as $t^{1/2}$ instead of $t^{2/3}$). This point, which also appears in $f(R)$ gravity, can exist as the only matter point for some models.

(vi) There is a stable de Sitter point that is the final attractor of the theory. This point appears in $f(R)$ gravity too, and exists provided that

$$0 < m < 1 \quad \text{at } r = -2.$$

The acceptable cosmological solutions must be a transition from a saddle radiation era to a saddle matter era and be able to be connected with an accelerated point as the final attractor, provided that the matter domination takes long enough to form cosmic structures. In principle, in this theory we have two matter points (one a "standard" and the other a "nonstandard" point), two accelerated points, and a de Sitter solution. Based on the existence of cosmological solutions, we classified the

acceptable solutions into six classes. Two of them have the fixed point P_1 as the final attractor, two have transitions to some regions of P_2, and for the last two P_8 acts as a de Sitter solution. All these classes of solutions are new ones with respect to $f(R, T)$ gravity, except when the corresponding models have P_8 as a final attractor. However, in $f(R, T)$ gravity P_8 can be reached after passing by P_1 for some periods. We briefly compared the properties of solutions in terms of acceptable transitions for several specific models in both $f(R, T)$ and $f(R)$ gravities in Table III. Numerically, we have shown that theories with $g(R) = aR^{-\beta}$, $g(R) = R^p \exp(qR)$, $g(R) = R + \alpha R^{-n}$, $g(R) = R^p[\log(\alpha R)]^q$, and $g(R) = R^p \exp(q/R)$ have proper sequences of the radiation-matter-acceleration eras for some values of their space parameters, which indicate that these theories deserve further investigation. We have shown that for the corresponding models, in which the cosmological trajectories advance to P_8, the trajectories pass by P_1 before approaching P_8. Also, we numerically checked that it is always possible to control the duration in which the trajectories stay around P_1 and the duration of the matter dominated era (the width of the matter-density parameter in the related diagrams).

In $f(R, T)$ gravity with the minimal coupling, our investigated models can present a standard cosmological history, including transient periods of radiation and matter domination followed by a period of accelerated expansion domination, which can also give the presently observed [87] contribution of the density parameters $\Omega_0^{(m)} \simeq 0.3$ and $\Omega_0^{(\mathrm{DE})} \simeq 0.7$. Some of the models can explain the accelerated expansion via a dark energy with an effective equation of state parameter of about -1. However, for some of the other models, the trajectories are trapped in the point P_1 and hence this effective parameter approaches the value $-1/2$, which contradicts the recent Planck results [87]. Also, our models numerically suggest a power–law behavior of the scale factors (near $z \simeq 0$) of the form $a(t) \propto t^n$ for $1.025 < n < 1.038$, which gives an accelerated epoch and leads to a Hubble parameter of the form $H(z) \propto (1 + z)^{1/n}$. These results were obtained numerically; however, a non-numeric analysis can be performed to reconstruct these models with constant parameters that are consistent with the present values of H_0 and $\Omega_0^{(m)}$. Beyond these preliminary considerations, one can also further constraint the models using the SNIa measurements, the distance to the baryonic acoustic oscillations and/or the position of the first peak in the spectrum of anisotropies of CMBR observation. Indeed, one can theoretically obtain the Hubble parameter $H(z)$ for each model (which in addition to H_0 and $\Omega_0^{(m)}$, it may be a function of the other constant parameters of the model) then, performs the related calculations (e.g., the distance modulus of a supernova at redshift z) using $H(z)$ and hence, compares statistically the results with the available data (e.g., the observed distance modulus of a supernova) to find out the best values of the parameters of the model. Also, by a further step one can consider the model at the level of perturbation. That is, by obtaining the effective gravitational constant (which, in general, depends on the constant parameters of the model) one can track the structure formation around the matter era and thus constrain the parameters of the model (e.g., the scalar perturbations have been considered for some models in Ref. [71]). In a further study of $f(R, T)$ gravity, and in an independent work, it would be our task to present the observational constraints for our models.

The pure nonminimal theory has a few problems, in terms of both fundamental and cosmological aspects. First of all, a Lagrangian with the property $h(T) = 0$ at $T = 0$ does not lead to the vacuum solution, and actually one gets a null Lagrangian. In addition, there is another problem in the cosmological regime, namely, there is lack of a matter point; that is, all the fixed points have $\Omega^{(m)} = 0$ (see Table IV for more details).

In the nonminimal theory, the corresponding fixed points consist of the following.

(i) The same matter point as the minimal theory, but with different eigenvalues. This point exists provided that $m \to 0^+$ and $m'(r) > -1$, which is the same as in $f(R)$ gravity.

(ii) Three fixed points as stable accelerated expansion solutions, which are

$$m'(r) < -1, \qquad 0.347 \lesssim m < 1/2,$$
$$-1/3 < w^{(\mathrm{eff})} < -0.260, \qquad m'(r) < -1,$$
$$0.486 \lesssim m < 0.60, \qquad -1 < w^{(\mathrm{eff})} \lesssim -0.75$$

in the nonphantom domain, and

$$m'(r) > -1, \qquad m > 0.60, \qquad w^{(\mathrm{eff})} < -1$$

in the phantom domain.

(iii) A stable de Sitter point which exists provided that $0 < m < 1/2$.

Further considerations of the possible transitions and studies of various models of this theory will be reported elsewhere.

ACKNOWLEDGMENTS

We thank the Research Office of Shahid Beheshti University G.C. for financial support.

[1] M. Farhoudi, Ph.D. thesis, Queen Mary and Westfield College, University of London, 1995.
[2] S. Capozziello and M. De Laurentis, Phys. Rep. **509**, 167 (2011).
[3] J. M. Overduin and P. S. Wesson, Phys. Rep. **283**, 303 (1997).
[4] R. Maartens, Living Rev. Relativity **7**, 7 (2004).
[5] V. Faraoni, *Cosmology in Scalar-Tensor Gravity* (Kluwer Academic Publishers, London, 2004).
[6] M. Farhoudi, Gen. Relativ. Gravit. **38**, 1261 (2006).
[7] S. Nojiri and S. D. Odintsov, Int. J. Geom. Methods Mod. Phys. **04**, 115 (2007).
[8] T. P. Sotiriou, Ph.D. thesis, International School for Advanced Studies, Trieste, 2007.
[9] A. De Felice and S. Tsujikawa, Living Rev. Relativity **13**, 3 (2010).
[10] T. P. Sotiriou and V. Faraoni, Rev. Mod. Phys. **82**, 451 (2010).
[11] S. Nojiri and S. D. Odintsov, Phys. Rep. **505**, 59 (2011).
[12] T. Clifton, P. G. Ferreira, A. Padilla, and C. Skordis, Phys. Rep. **513**, 1 (2012).
[13] G. Bertonea, D. Hooperb, and J. Silk, Phys. Rep. **405**, 279 (2005).
[14] J. Silk, Ann. Phys. (Berlin) **15**, 75 (2006).
[15] J. L. Feng, Annu. Rev. Astron. Astrophys. **48**, 495 (2010).
[16] C. S. Frenk and S. D. M. White, Ann. Phys. (Berlin) **524**, 507 (2012).
[17] L. Bergström, Ann. Phys. (Berlin) **524**, 479 (2012).
[18] P. J. E. Peebles, Rev. Mod. Phys. **75**, 559 (2003).
[19] D. Polarski, Ann. Phys. (Berlin) **15**, 342 (2006).
[20] E. J. Copeland, M. Sami, and S. Tsujikawa, Int. J. Mod. Phys. D **15**, 1753 (2006).
[21] R. Durrer and R. Maartens, Gen. Relativ. Gravit. **40**, 301 (2008).
[22] K. Bamba, S. Capozziello, S. Nojiri, and S. D. Odintsov, Astrophys. Space Sci. **342**, 155 (2012).
[23] M. Persic, P. Salucci, and F. Stel, Mon. Not. R. Astron. Soc. **281**, 27 (1996).
[24] B. Catinella, R. Giovanelli, and M. P. Haynes, Astrophys. J. **640**, 751 (2006).
[25] S. Weinberg, *Cosmology* (Oxford University Press, New York, 2008).
[26] A. H. Guth, Phys. Rev. D **23**, 347 (1981).
[27] A. D. Linde, Phys. Lett. B **108**, 389 (1982).
[28] A. D. Linde, Phys. Lett. B **129**, 177 (1983).
[29] A. D. Linde, Rep. Prog. Phys. **47**, 925 (1984).
[30] R. H. Brandenberger, arXiv:hep-ph/0101119.
[31] A. G. Riess *et al.*, Astron. J. **116**, 1009 (1998).
[32] S. Perlmutter *et al.*, Astrophys. J. **517**, 565 (1999).
[33] A. G. Riess *et al.*, Astron. J. **117**, 707 (1999).
[34] J. L. Tonry *et al.*, Astrophys. J. **594**, 1 (2003).
[35] R. A. Knop *et al.*, Astrophys. J. **598**, 102 (2003).
[36] M. Tegmark *et al.* (SDSS Collaboration), Phys. Rev. D **69**, 103501 (2004).
[37] M. Tegmark *et al.* (SDSS Collaboration), Phys. Rev. D **74**, 123507 (2006).
[38] D. J. Eisenstein *et al.* (SDSS Collaboration), Astrophys. J. **633**, 560 (2005).
[39] C. Blake, D. Parkinson, B. Bassett, K. Glazebrook, M. Kunz, and R. C. Nichol, Mon. Not. R. Astron. Soc. **365**, 255 (2006).
[40] W. J. Percival, S. Cole, D. J. Eisenstein, R. C. Nichol, J. A. Peacock, A. C. Pope, and A. S. Szalay, Mon. Not. R. Astron. Soc. **381**, 1053 (2007).
[41] D. N. Spergel *et al.* (WMAP Collaboration), Astrophys. J. Suppl. Ser. **148**, 175 (2003).
[42] D. N. Spergel *et al.* (WMAP Collaboration), Astrophys. J. Suppl. Ser. **170**, 377 (2007).
[43] E. Komastu *et al.* (WMAP Collaboration), Astrophys. J. Suppl. Ser. **180**, 330 (2009).
[44] B. Jain and A. Taylor, Phys. Rev. Lett. **91**, 141302 (2003).
[45] T. Damour, Classical Quantum Gravity **9**, S55 (1992).
[46] C. M. Will, *Theory and Experiment in Gravitational Physics* (Cambridge University Press, New York, 1993).
[47] S. G. Turyshev, Phys. Usp. **52**, 1 (2009).
[48] L. Iorio, H. I. M. Lichtenegger, M. L. Ruggiero, and C. Corda, Astrophys. Space Sci. **331**, 351 (2011).
[49] N. D. Birrell and P. C. W. Davies, *Quantum Fields in Curved Space* (Cambridge University Press, New York, 1982).
[50] I. L. Buchbinder, S. D. Odintsov, and I. L. Shapiro, *Effective Action in Quantum Gravity* (Institute of Physics Publishing, Bristol, 1992).
[51] R. Utiyama and B. S. Dewitt, J. Math. Phys. (N.Y.) **3**, 608 (1962).
[52] E. Pechlaner and R. Sexl, Commun. Math. Phys. **2**, 165 (1966).
[53] J. P. Ostriker and P. J. Steinhardt, arXiv:astro-ph/9505066.
[54] H. Padmanabhan and T. Padmanabhan, Int. J. Mod. Phys. D **22**, 1342001 (2013).
[55] D. Bernard and A. LeClair, Phys. Rev. D **87**, 063010 (2013).
[56] S. Nobbenhuis, arXiv:gr-qc/0609011.
[57] T. Chiba, T. Okabe, and M. Yamaguchi, Phys. Rev. D **62**, 023511 (2000).
[58] C. Armendariz-Picon, V. Mukhanov, and P. J. Steinhardt, Phys. Rev. Lett. **85**, 4438 (2000).
[59] T. Chiba, Phys. Lett. B **575**, 1 (2003).
[60] A. D. Dolgova and M. Kawasaki, Phys. Lett. B **573**, 1 (2003).
[61] A. L. Erickcek, T. L. Smith, and M. Kamionkowski, Phys. Rev. D **74**, 121501 (2006).
[62] B. Li and J. D. Barrow, Phys. Rev. D **75**, 084010 (2007).
[63] T. Harko, F. S. N. Lobo, S. Nojiri, and S. D. Odintsov, Phys. Rev. D **84**, 024020 (2011).
[64] M. J. S. Houndjo, Int. J. Mod. Phys. D **21**, 1250003 (2012).
[65] F. G. Alvarenga, M. J. S. Houndjo, A. V. Monwanou, and J. B. Chabi Orou, J. Mod. Phys. **04**, 130 (2013).
[66] M. J. S. Houndjo, arXiv:1207.1646.
[67] M. Sharif and M. Zubair, J. Cosmol. Astropart. Phys. 03 (2012) 028.
[68] M. Jamil, D. Momeni, and M. Ratbay, Chin. Phys. Lett. **29**, 109801 (2012).
[69] S. M. Farasat, A. Jhangeer, and A. A. Bhatti, arXiv:1207.0708.
[70] M. Jamil, D. Momeni, R. Muhammad, and M. Ratbay, Eur. Phys. J. C **72**, 1999 (2012).
[71] F. G. Alvarenga, A. de la Cruz-Dombriz, M. J. S. Houndjo, M. E. Rodrigues, and D. Sáez-Gómez, Phys. Rev. D **87**, 103526 (2013).
[72] M. Farhoudi, Int. J. Mod. Phys. D **14**, 1233 (2005).

[73] S. D. Odintsov and D. Sáez-Gómez, arXiv:1304.5411.
[74] Z. Haghani, T. Harko, F. S. N. Lobo, H. R. Sepangi, and S. Shahidi, Phys. Rev. D **88**, 044023 (2013).
[75] L. Iorio and E. N. Saridakis, Mon. Not. R. Astron. Soc. **427**, 1555 (2012).
[76] L. Amendola, R. Gannouji, D. Polarski, and S. Tsujikawa, Phys. Rev. D **75**, 083504 (2007).
[77] D. Lovelock and H. Rund, *Tensors, Differential Forms and Variational Principles* (Wiley, New York, 1975).
[78] R. d'Inverno, *Introducing Einstein's Relativity* (Clarendon Press, Oxford, 1992).
[79] *Dynamical Systems in Cosmology*, edited by J. Wainwright and G. F. R. Ellis (Cambridge University Press, New York, 1997).
[80] H. Farajollahi and A. Salehi, J. Cosmol. Astropart. Phys. 11 (2010) 006.
[81] H. Farajollahi and A. Salehi, J. Cosmol. Astropart. Phys. 07 (2011) 036.
[82] Z. Haghani, H. R. Sepangi, and S. Shahidi, J. Cosmol. Astropart. Phys. 02 (2012) 031.
[83] L. Amendola, D. Polarski, and S. Tsujikawa, Phys. Rev. Lett. **98**, 131302 (2007).
[84] L. Amendola, D. Polarski, and S. Tsujikawa, Int. J. Mod. Phys. D **16**, 1555 (2007).
[85] M. Abdelwahab, S. Carloni, and P. K. S. Dunsby, Classical Quantum Gravity **25**, 135002 (2008).
[86] L. Amendola, Phys. Rev. D **62**, 043511 (2000).
[87] P. A. R. Ade *et al.*, arXiv:1303.5076.